OCM, and *LMTK2* and we considered *LMTK2* worthy of attention. LMTK2 is a transmembrane protein which possesses serine/threonine kinase activity [Wang and Brautigan, 2002]. It is expressed predominantly in skeletal muscle [Wang and Brautigan, 2002]. The knockout mouse showed no limb abnormalities but azoospermia [Kawa et al., 2006]. As no *LMTK2* mutations were observed in 29 SHFM patients without hearing loss, it may be interesting to investigate *LMTK2* mutations particularly in SHFM1D.

The 4.6-Mb deletion at 15q21.1-q21.2 encompassed 21 RefSeq genes. We could not exclude the possibility that the deletion of these genes may contribute to the patient's phenotype including SHFM, though any known SHFM loci are not associated with 15q21. It should be noted that *FBN1* was completely deleted. Haploinsufficiency of *FBN1* could be involved in pathogenesis of Marfan syndrome [Mizuguchi and Matsumoto, 2007], but the patient did not show any Marfan syndrome features.

In conclusion, the complex 7q21.3 rearrangement in the SHFM1D patient was intensively analyzed. Microarray analysis may potentially add novel findings leading to full understanding of SHFM1D and/or SHFM.

ACKNOWLEDGMENTS

We thank patients and their families for their participation in this study. This study was supported by a research grant from the Ministry of Health, Labour and Welfare (N.M.) and SORST from JST (N.M.).

REFERENCES

Ahmad M, Abbas H, Haque S, Flatz G. 1987. X-chromosomally inherited split-hand/split-foot anomaly in a Pakistani kindred. Hum Genet 75: 169–173.

Boles RG, Pober BR, Gibson LH, Willis CR, McGrath J, Roberts DJ, Yang-Feng TL. 1995. Deletion of chromosome 2q24-q31 causes characteristic digital anomalies: Case report and review. Am J Med Genet 55:155–160.

Celli J, Duijf P, Hamel BC, Bamshad M, Kramer B, Smits AP, Newbury-Ecob R, Hennekam RC, Van Buggenhout G, van Haeringen A, Woods CG, van Essen AJ, de Waal R, Vriend G, Haber DA, Yang A, McKeon F, Brunner HG, van Bokhoven H. 1999. Heterozygous germline mutations in the p53 homolog p63 are the cause of EEC syndrome. Cell 99:143–153.

Crackower MA, Scherer SW, Rommens JM, Hui CC, Poorkaj P, Soder S, Cobben JM, Hudgins L, Evans JP, Tsui LC. 1996. Characterization of the split hand/split foot malformation locus SHFM1 at 7q21.3-q22.1 and analysis of a candidate gene for its expression during limb development. Hum Mol Genet 5:571–579.

Duijf PHG, van Bokhoven H, Brunner HG. 2003. Pathogenesis of split-hand/split-foot malformation. Hum Mol Genet 12:R51–R60.

Elliott AM, Evans JA. 2006. Genotype-phenotype correlations in mapped split hand foot malformation (SHFM) patients. Am J Med Genet Part A 140A:1419–1427.

Elliott AM, Evans JA, Chudley AE. 2005. Split hand foot malformation (SHFM). Clin Genet 68:501–505.

Faiyaz-Ul-Haque M, Zaidi SH, King LM, Haque S, Patel M, Ahmad M, Siddique T, Ahmad W, Tsui LC, Cohn DH. 2005. Fine mapping of the X-linked split-hand/split-foot malformation (SHFM2) locus to a 5.1-Mb region on Xq26.3 and analysis of candidate genes. Clin Genet 67: 93–97.

Goodman FR, Majewski F, Collins AL, Scambler PJ. 2002. A 117-kb microdeletion removing HOXD9-HOXD13 and EVX2 causes synpolydactyly. Am J Hum Genet 70:547–555.

Gurnett CA, Dobbs MB, Nordsieck EJ, Keppel C, Goldfarb CA, Morcuende JA, Bowcock AM. 2006. Evidence for an additional locus for split hand/foot malformation in chromosome region 8q21.11-q22.3. Am J Med Genet Part A 140A:1744–1748.

Gurrieri F, Prinos P, Tackels D, Kilpatrick MW, Allanson J, Genuardi M, Vuckov A, Nanni L, Sangiorgi E, Garofalo G, Nunes ME, Neri G, Schwartz C, Tsipouras P. 1996. A split hand-split foot (SHFM3) gene is located at 10q24–>25. Am J Med Genet 62:427–436.

Ianakiev P, Kilpatrick MW, Toudjarska I, Basel D, Beighton P, Tsipouras P. 2000. Split-hand/split-foot malformation is caused by mutations in the p63 gene on 3q27. Am J Hum Genet 67:59–66.

Kano H, Kurosawa K, Horii E, Ikegawa S, Yoshikawa H, Kurahashi H, Toda T. 2005. Genomic rearrangement at 10q24 in non-syndromic split-hand/split-foot malformation. Hum Genet 118:477–483.

Kawa S, Ito C, Toyama Y, Maekawa M, Tezuka T, Nakamura T, Nakazawa T, Yokoyama K, Yoshida N, Toshimori K, Yamamoto T. 2006. Azoospermia in mice with targeted disruption of the Brek/Lmtk2 (brain-enriched kinase/lemur tyrosine kinase 2) gene. Proc Natl Acad Sci 103:19344–19349.

Lo Iacono N, Mantero S, Chiarelli A, Garcia E, Mills AA, Morasso MI, Costanzo A, Levi G, Guerrini L, Merlo GR, 2008. Regulation of Dlx5 and Dlx6 gene expression by p63 is involved in EEC and SHFM congenital limb defects. Development 135:1377–1388.

Mizuguchi T, Matsumoto N. 2007. Recent progress in genetics of Marfan syndrome and Marfan-associated disorders. J Hum Genet 52:1–12.

Nannya Y, Sanada M, Nakazaki K, Hosoya N, Wang L, Hangaishi A, Kurokawa M, Chiba S, Bailey DK, Kennedy GC, Ogawa S. 2005. A robust algorithm for copy number detection using high-density oligonucleotide single nucleotide polymorphism genotyping arrays. Cancer Res 65: 6071–6079.

Nunes ME, Schutt G, Kapur RP, Luthardt F, Kukolich M, Byers P, Evans JP. 1995. A second autosomal split hand/split foot locus maps to chromosome 10q24-q25. Hum Mol Genet 4:2165–2170.

Raas-Rothschild A, Manouvrier S, Gonzales M, Farriaux JP, Lyonnet S, Munnich A. 1996. Refined mapping of a gene for split hand-split foot malformation (SHFM3) on chromosome 10q25. J Med Genet 33: 996–1001.

Robledo RF, Rajan L, Li X, Lufkin T. 2002. The Dlx5 and Dlx6 homeobox genes are essential for craniofacial, axial, and appendicular skeletal development. Genes Dev 16:1089–1101.

Saitsu H, Kato M, Mizuguchi T, Hamada K, Osaka H, Tohyama J, Uruno K, Kumada S, Nishiyama K, Nishimura A, Okada I, Yoshimura Y, Hirai S, Kumada T, Hayasaka K, Fukuda A, Ogata K, Matsumoto N. 2008. De novo mutations in the gene encoding STXBP1 (MUNC18–1) cause early infantile epileptic encephalopathy. Nat Genet 40:782–788.

Scherer SW, Poorkaj P, Allen T, Kim J, Geshuri D, Nunes M, Soder S, Stephens K, Pagon RA, Patton MA, et al. 1994a. Fine mapping of the autosomal dominant split hand/split foot locus on chromosome 7, band q21.3-q22.1. Am J Hum Genet 55:12–20.

Scherer SW, Poorkaj P, Massa H, Soder S, Allen T, Nunes M, Geshuri D, Wong E, Belloni E, Little S, et al. 1994b. Physical mapping of the split hand/split foot locus on chromosome 7 and implication in syndromic ectrodactyly. Hum Mol Genet 3:1345–1354.

Scherer SW, Cheung J, MacDonald JR, Osborne LR, Nakabayashi K, Herbrick JA, Carson AR, Parker-Katiraee L, Skaug J, Khaja R, Zhang

J, Hudek AK, Li M, Haddad M, Duggan GE, Fernandez BA, Kanematsu E, Gentles S, Christopoulos CC, Choufani S, Kwasnicka D, Zheng XH, Lai Z, Nusskern D, Zhang Q, Gu Z, Lu F, Zeesman S, Nowaczyk MJ, Teshima I, Chitayat D, Shuman C, Weksberg R, Zackai EH, Grebe TA, Cox SR, Kirkpatrick SJ, Rahman N, Friedman JM, Heng HH, Pelicci PG, Lo-Coco F, Belloni E, Shaffer LG, Pober B, Morton CC, Gusella JF, Bruns GA, Korf BR, Quade BJ, Ligon AH, Ferguson H, Higgins AW, Leach NT, Herrick SR, Lemyre E, Farra CG, Kim HG, Summers AM, Gripp KW, Roberts W, Szatmari P, Winsor EJ, Grzeschik KH, Teebi A, Minassian BA, Kere J, Armengol L, Pujana MA, Estivill X, Wilson MD, Koop BF, Tosi S, Moore GE, Boright AP, Zlotorynski E, Kerem B, Kroisel PM, Petek E, Oscier DG, Mould SJ, Dohner H, Dohner K, Rommens JM, Vincent JB, Venter JC, Li PW, Mural RJ, Adams MD, Tsui LC. 2003. Human chromosome 7: DNA sequence and biology. Science 300: 767–772.

Ugur SA, Tolun A. 2008. Homozygous WNT10b mutation and complex inheritance in split hand foot malformation. Hum Mol Genet 17: 2644–2653.

van Bokhoven H, Hamel BC, Bamshad M, Sangiorgi E, Gurrieri F, Duijf PH, Vanmolkot KR, van Beusekom E, van Beersum SE, Celli J, Merkx GF, Tenconi R, Fryns JP, Verloes A, Newbury-Ecob RA, Raas-Rotschild A, Majewski F, Beemer FA, Janecke A, Chitayat D, Crisponi G, Kayserili H, Yates JR, Neri G, Brunner HG. 2001. p63 Gene mutations in eec syndrome, limb-mammary syndrome, and isolated split hand-split foot malformation suggest a genotype-phenotype correlation. Am J Hum Genet 69:481–492.

Wang H, Brautigan DL. 2002. A Novel transmembrane Ser/Thr kinase complexes with protein phosphatase-1 and inhibitor-2. J Biol Chem 277:49605–49612.

Journal of the Neurological Sciences 290 (2010) 172–176

Contents lists available at ScienceDirect

Journal of the Neurological Sciences

journal homepage: www.elsevier.com/locate/jns

Short communication

Siblings with the adult-onset slowly progressive type of pantothenate kinase-associated neurodegeneration and a novel mutation, Ile346Ser, in *PANK2*: Clinical features and ^{99m}Tc-ECD brain perfusion SPECT findings

Hiroshi Doi [a,*], Shigeru Koyano [a], Satoko Miyatake [b], Naomichi Matsumoto [b], Tomoaki Kameda [a], Atsuko Tomita [a], Yosuke Miyaji [a], Yume Suzuki [a], Yukio Sawaishi [c], Yoshiyuki Kuroiwa [a]

[a] Department of Clinical Neurology and Stroke Medicine, Graduate School of Medical Sciences, Yokohama City University, Japan
[b] Department of Human Genetics, Graduate School of Medical Sciences, Yokohama City University, Japan
[c] Department of Pediatrics, Graduate School of Medicine, Akita University, Japan

ARTICLE INFO

Article history:
Received 31 July 2009
Received in revised form 22 October 2009
Accepted 17 November 2009
Available online 14 December 2009

Keywords:
Neuroimaging
Neurogenetics
Pantothenate kinase-associated neurodegeneration
Pantothenate kinase 2 gene (*PANK2*)
Hallervorden–Spatz syndrome

ABSTRACT

Pantothenate kinase-associated neurodegeneration (PKAN), formerly known as Hallervorden–Spatz syndrome (HSS), is an autosomal recessive neurodegenerative disorder characterized by iron accumulation in the brain. Mutations in the pantothenate kinase 2 (*PANK2*) gene are known to be responsible for PKAN. Several studies have revealed correlations between clinical phenotypes and particular *PANK2* mutations. The adult-onset slowly progressive type of PKAN with *PANK2* mutations is very rare. In this report, we describe siblings with the adult-onset slowly progressive type of PKAN with a novel mutation, Ile346Ser, in *PANK2*. The siblings had the same mutation in *PANK2* and had common clinical signs such as misalignment of teeth, a high arched palate, hollow feet, a slight cognitive decline, and an apparent executive dysfunction, although they showed different patterns of movement disorders. Thus, even if PKAN patients have identical mutations, it is likely that they will present with different types of movement disorders. Brain perfusion single photon emission computed tomography in both patients showed decreased regional cerebral blood flow in the bilateral frontoparietal lobes, the globus pallidus, the striatum, and around the ventriculus quartus. Cardiac uptake of [^{123}I] meta-iodobenzylguanidine was normal in both patients. Analysis of genotype–phenotype correlations and the elucidation of mutational effects on pantothenate kinase 2 function, expression, and structure are important for understanding the mechanisms of PKAN.

1. Introduction

Pantothenate kinase-associated neurodegeneration (PKAN), formerly known as Hallervorden–Spatz syndrome (HSS), is an autosomal recessive neurodegenerative disorder characterized by iron accumulation in the globus pallidus and the substantia nigra, with axonal swellings in nuclei of those brain regions and throughout the cortex [1,2]. Patients with PKAN are classified into three groups: 1) an early-onset childhood type (those with an evident diagnosis before 10 years of age), which includes both rapidly and slowly progressive types, 2) a late-onset slowly progressive type (those with an evident diagnosis after 10 years of age and before 18 years of age), and 3) an adult-onset slowly progressive type [3]. Clinical phenotypes include progressive extrapyramidal dysfunction presenting as dystonia, rigidity, choreoathetosis, dysarthria, and gait disturbance. Retinitis pigmentosa, optic atrophy, and intellectual retardation or decline are also common in the early-onset childhood type [1,3]. After mutations in the pantothenate kinase 2 (*PANK2*) gene were found to be responsible for HSS [4], several studies revealed significant correlations between clinical phenotypes and types of *PANK2* mutations [4–20]. Among those studies, only four reports have described the detailed clinical features of the adult-onset slowly progressive type of PKAN with *PANK2* mutations [13,14,17,18].

In this report, we describe two Japanese siblings with the adult-onset slowly progressive type of PKAN who were found to have a novel *PANK2* mutation.

2. Patients

The family pedigree is shown in Fig. 1A. The patients were the first and second of three children of a Japanese consanguineous couple.

2.1. Case 1

This right-handed man had an unremarkable birth and developmental history. At 28 years of age, his right arm developed sensations

* Corresponding author. Department of Clinical Neurology and Stroke Medicine, Yokohama City University, 3-9 Fukuura, Kanazawa-ku, Yokohama 234-0006, Japan. Tel.: +81 45 787 2725; fax: +81 45 788 6041.
E-mail address: doi@rkd.d-bs.com (H. Doi).

0022-510X/$ – see front matter © 2009 Elsevier B.V. All rights reserved.
doi:10.1016/j.jns.2009.11.008

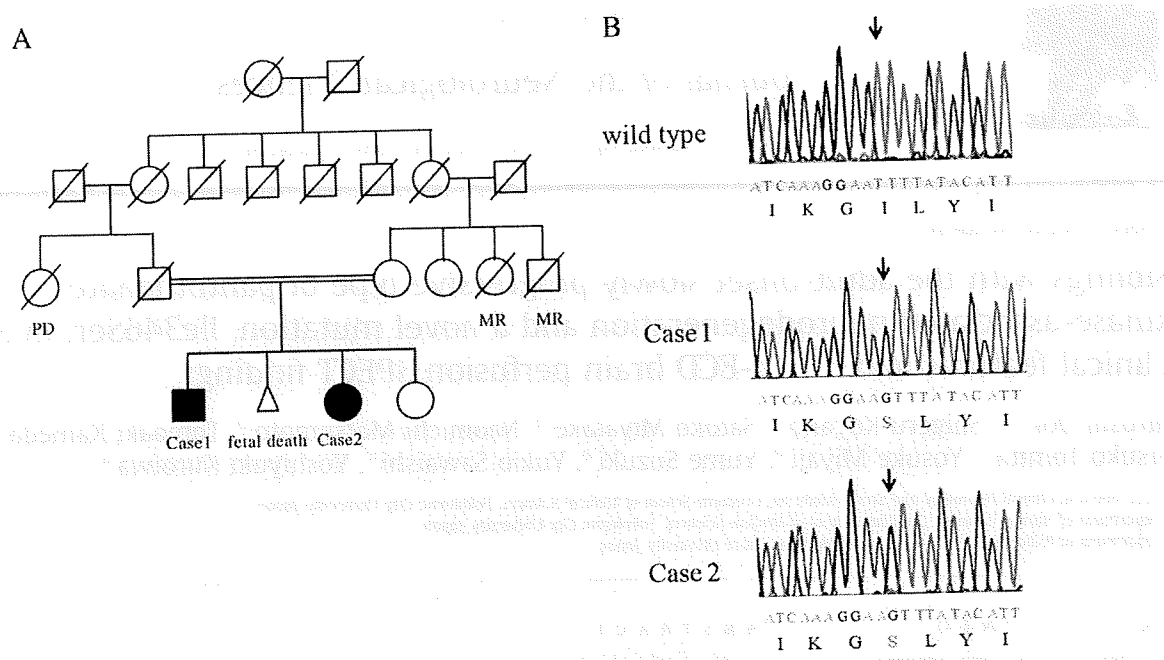

Fig. 1. A. Pedigree of the family. PD: Parkinson disease, MR: mental retardation. B. Sequence analysis of *PANK2* in the patients. A homozygous 1037T>G point mutation (arrows) and the resulting Ile342Ser amino acid substitution were found in both patients.

of freezing when he used a food chopper. At 32 years of age, he noticed the same feeling in his left arm, and he could not continue to work as a cook. Around 40 years of age, he noticed difficulty in articulating properly and in swallowing water in one gulp. He sometimes bit his tongue while eating because he could not chew food well. Around the same time, he sometimes felt awkward walking. These symptoms gradually worsened, and he visited our hospital at 57 years of age. A physical examination revealed misalignment of teeth with an asymmetrical line, a high arched palate, and hollow feet. He did not show psychiatric features such as delusions, hallucinations, agitation, depression, apathy, anxiety, or irritability. A neurological examination showed a slight cognitive decline. His mini-mental state examination (MMSE) score was 28/30. The frontal assessment battery [21] (FAB) score was 14/18, indicating that he had slight frontal lobe dysfunction. The times required to complete the Japanese version of the Trail Making Test Part A (TMT A) and Part B (TMT B) [22] were 30 s and 90 s, respectively. Using the 48-card procedure of the Wisconsin Card Sorting Test (WCST), this patient made 33 errors, including eight perseverative errors of Nelson type [23]. The number of category achieved (CA) was 0, indicating that he had an apparent executive dysfunction.

He showed no signs of aphasia, apraxia, or agnosia; however, he did show dysarthria, dysphagia, and mild rigidity in the extremities, and resting tremor in his right fingers. His laboratory tests were normal except for acanthocytosis. An electrocardiogram (ECG) showed abnormal findings consistent with Wolff–Parkinson–White syndrome. An electroencephalogram (EEG) and a nerve conduction study (NCS) were normal.

2.2. Case 2

This left-handed woman had an unremarkable birth history. She had primary amenorrhea and was diagnosed with diabetes mellitus at 25 years of age. She underwent surgery to remove a sigmoid colon cancer at 33 years of age. At 35 years of age, she experienced involuntary movement of her right arm, and she sometimes spilled soup or drinks. At 43 years of age, she began to feel pain in her right foot, and her second to fifth toes were fixed in a flexed position. As these symptoms gradually worsened, she visited our hospital at 53 years of age. Physical examination revealed misalignment of teeth, a high arched palate, and hollow feet. She did not show psychiatric features such as delusions, hallucinations, agitation, depression, apathy, anxiety, or irritability. A neurological examination showed a slight cognitive decline. Her MMSE score was 28/30. Her FAB score was 12/18, indicating that she had slight frontal lobe dysfunction. The times required to complete the TMT A and TMT B were 40 s and 150 s, respectively. Using the WCST, this patient made 35 errors, including 12 perseverative errors of Nelson type. The CA was 0, indicating that she had an apparent executive dysfunction.

She had no aphasia, apraxia, or agnosia. She did not show dysarthria, dysphagia, or rigidity in the extremities, but she did show focal dystonia in the right toes, chorea in the upper limbs, and slight spasticity in the lower limbs. Her vibration sense in the lower limbs was mildly decreased, probably due to diabetic neuropathy. Her laboratory tests were normal except for acanthocytosis and a high level of serum Hb_{A1c}. An EEG was normal. An NCS showed a slight decrease in motor and sensory nerve conduction velocity, consistent with diabetic neuropathy.

The clinical features of the siblings are summarized in Table 1.

3. Radiological findings

Magnetic resonance imaging (MRI) revealed central hyperintensity within the hypointense medial globus pallidus on T2 weighted image ('eye-of-the-tiger' sign [24]) in both patients (Fig. 2A). Brain perfusion single photon emission computed tomography (SPECT) using [^{99m}Tc] ethyl cysteinate dimer (^{99m}Tc-ECD) in both patients showed decreased regional cerebral blood flow (rCBF) in the bilateral frontoparietal lobes, the globus pallidus, the striatum, and around the ventriculus quartus (Fig. 2B). To evaluate rCBF, we adopted an easy *Z*-score imaging system (eZIS) with which changes in rCBF during the early stages of neurodegenerative diseases could be assessed [25]. With the eZIS, each SPECT image of the patients was anatomically standardized and compared to the mean and standard

Table 1
Summary of clinical features of the patients.

	Case 1	Case 2
Age of onset	28	35
Misalignment of the teeth	+	+
Hollow feet	+	±
Cognitive decline and executive dysfunction	+	+
Dysarthria	+	−
Dysphagia	+	−
Tremor	+	−
Chorea	−	+
Focal dystonia	−	+
Postural instability	+	−
Pyramidal sign	−	+
Acanthocytosis	+	+
'Eye-of-the-tiger' sign	+	+
PANK2 mutation	I346S, homozygous	I346S, homozygous
Others	WPW syndrome	Diabetes mellitus Colon cancer Primary amenorrea

WPW: Wolff–Parkinson–White syndrome.

deviation (SD) of SPECT images of 30 age-matched healthy volunteers from 40 to 59 years old, which had previously been incorporated into the eZIS program as normal controls. Voxel-by-voxel Z-score analysis was performed after voxel normalization to global mean values: Z-score = (control mean − individual value)/(control SD) [25,26]. We also performed [^{123}I] meta-iodobenzylguanidine (^{123}I-MIBG) myocardial scintigraphy in both patients. The ratio of heart to mediastinum MIBG accumulation (H/M) was determined at 20 min and 4 h after administration of MIBG. The early and late H/M were 2.73 and 2.73 in case 1, and 2.31 and 2.40 in case 2, respectively, indicating that their cardiac sympathetic nerve function was intact.

4. Analysis of *PANK2*

After informed consent was obtained, genomic DNA was extracted from peripheral blood samples from these two patients, and we screened the entire coding sequence for *PANK2* mutations. We found a previously unreported homozygous missense mutation, Ile346Ser (1037T>G), in *PANK2* of both patients (Fig. 1B). Genomic DNA from 100 healthy Japanese controls was amplified using Genomiphi version 2 (GE healthcare). Mutation screening of exon 3 of *PANK2* including the novel mutation site was performed using high resolution melt analysis on a LightCycler480 apparatus (version 1.5.0; Roche Diagnostics). Two series of high resolution melt analyses were performed with and without 50% spike-in reference DNA from known homozygous alleles (wild type). The spike-in method allows one to more easily and more clearly distinguish a rare homozygous allele from a common homozygous allele than the standard method (without spike-DNA). Because all control DNAs were mixed with an equal amount of reference DNA, samples with rare homozygous alleles showed a distinct heterozygous melting curve pattern. We used the genomic DNA of case 2 as the positive control for homozygous mutant alleles, and the mixture of genomic DNA of case 2 and the reference DNA showed a clear heterozygous pattern. We compared all melting curves of normal control samples to that of the positive control. If samples showed any aberrant melting curve patterns, the forward and reverse strands were sequenced. Our results showed no Ile346Ser mutation in 100 normal controls (200 alleles).

5. Discussion

We describe siblings with the adult-onset slowly progressive type of PKAN with a novel mutation, Ile346Ser, in *PANK2*. To date, 77 types of *PANK2* mutations have been reported as being responsible for PKAN, including 47 types of missense mutations, nine types of nonsense mutations, 13 frameshift mutations, six mutations causing aberrant splicing, and two mutations causing an amino acid deletion [4–20]. In an extensive study on correlations between HSS phenotype and genotype in which an early-onset rapidly progressive childhood type was classified as a classic form, and other types of HSS were classified as an atypical form, it was shown that all patients with classic HSS and one third of those with atypical HSS had *PANK2* mutations [5]. PKAN patients can be distinguished from atypical HSS patients without *PANK2* mutations by examining an MRI image for the 'eye-of-the-tiger' sign, which is specific to patients with mutations in *PANK2* [5,24]. These studies indicate that patients who had been previously diagnosed with atypical HSS without the 'eye-of-the-tiger' sign on MRI tests did not always have *PANK2* mutations. However, there is one case report describing a classic HSS case with a *PANK2* mutation in which the 'eye-of-the-tiger' sign was initially present, but vanished during the course of the disease, suggesting that there is not a strict one to one correlation between the presence of the 'eye-of-the-tiger' sign and a *PANK2* mutation [19]. Therefore, it is important for clinicians to investigate patients with clinical features of atypical extrapyramidal disorders, focusing on *PANK2* mutations.

Among previous reports of PKAN cases, only four have described clinical features of an adult-onset slowly progressive type of PKAN with *PANK2* mutations [13,14,17,18]. Those cases were initially recognized as exhibiting essential tremor [13], amyotrophic lateral sclerosis [14], focal dystonia [18], or psychiatric disorders [17]. These cases had compound heterozygous missense mutations, homozygous missense mutations, or compound heterozygous nonsense and missense mutations in *PANK2*. Previous reports revealed that patients with the early-onset rapidly progressive type of PKAN had various types of *PANK2* mutations including truncating mutations, and that most patients with the other types of PKAN had missense mutations [5,16]. These results are in agreement with our hypothesis that the homozygous *PANK2* missense mutation found in our cases is a causative factor of an adult-onset slowly progressive type of PKAN. The siblings shared a common mutation in *PANK2* and had some common clinical features such as misalignment of teeth, a high arched palate, and hollow feet. The siblings also had a slight cognitive decline. As described above, scores of the TMT A and B in case 1 and TMT A in case 2 were considered to be within the normal range [27,28]. A difference between TMT A and TMT B (TMT B − A), which reflect cognitive flexibility independent of motor function, were considered abnormal in case 2 [29]. The WCST in both cases showed a high ratio of errors compared to normal control [23,28]. Both cases showed no apparent cognitive decline as measured by MMSE, but the FAB and WCST tests revealed that their executive functions were apparently impaired. On the other hand, the two patients showed different patterns of movement disorders. While the case 1 patient suffered from dysarthria, dysphasia, and gait disturbances, the case 2 patient did not show these symptoms. The prominent movement disorder in the case 2 patient was chorea of the upper limbs. It has been shown that pathologically corroborated HSS patients show diverse symptoms [1], and that PKAN patients with various *PANK2* mutations show diverse symptoms [16]. Our cases indicate that even when PKAN patients have identical mutations, they can present with different types of movement disorders. We conclude that there is no correlation between the type of mutation and the presence of movement disorders. On the other hand, neuroradiological findings showing the 'eye-of-the-tiger' sign on MRI were similar in both cases. Using ^{99m}Tc-ECD brain perfusion SPECT with the eZIS, which has been known to detect specific changes in rCBF in early stages of neurodegenerative diseases [25], we showed a decrease in rCBF in the bilateral frontoparietal lobes, the globus pallidus, the striatum, and around the ventriculus quartus. In early-onset childhood HSS cases, cerebellar hypoperfusion as shown with brain perfusion SPECT [30], and striatal and pontocerebellar hypoperfusion as shown with [^{15}O]-water positron emission

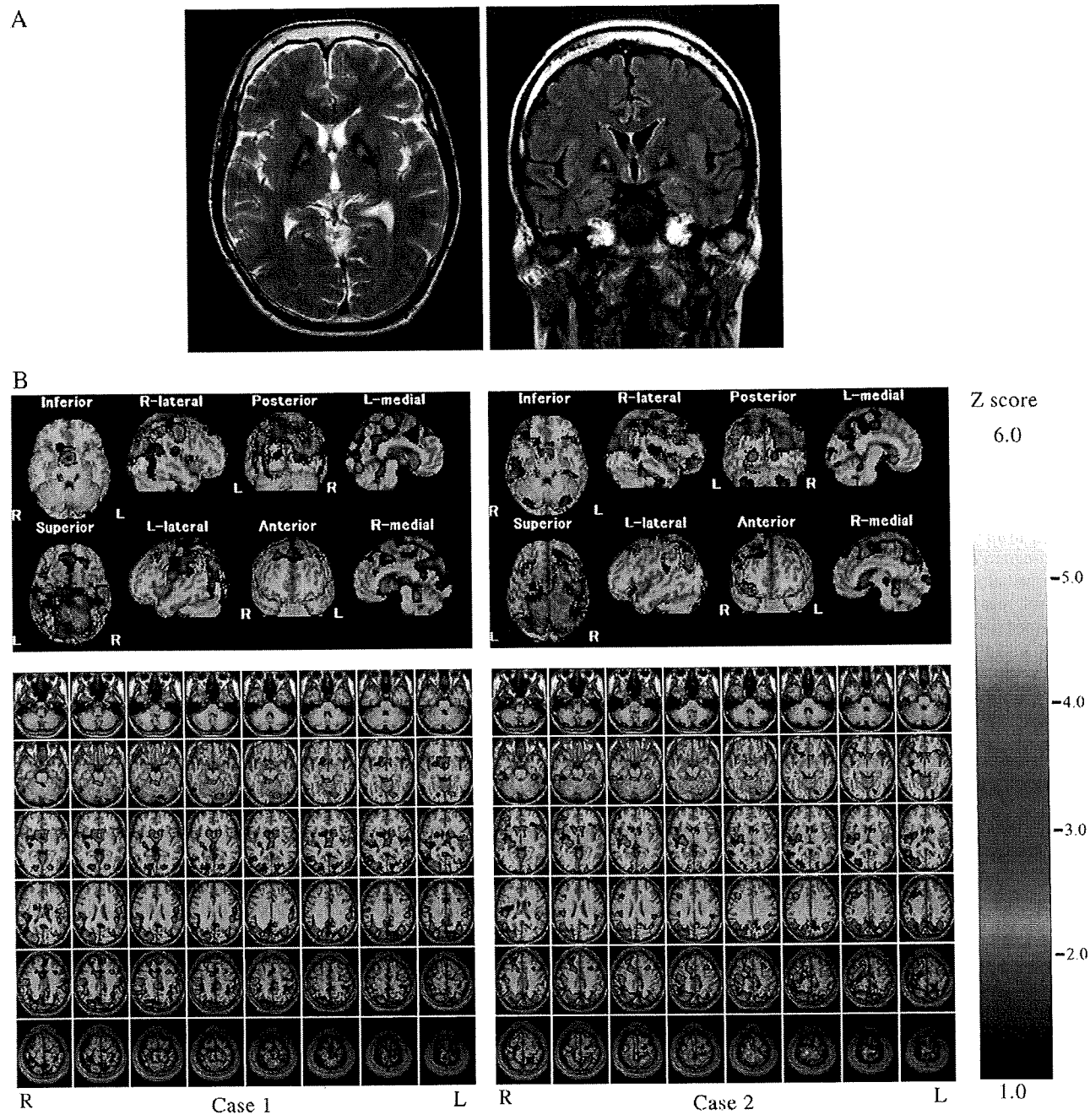

Fig. 2. Neuroradiological findings. A. MRI findings in the case 2 patient. An axial section of a T2 weighted image (left) and a coronal section of fluid attenuated inversion recovery image (right) are shown. Note that the MRI shows no brain atrophy. B. ^{99m}Tc-ECD SPECT in both cases. The Z-score maps displayed on an anatomically standardized MRI template are shown.

tomography [31] have been reported. Our cases showed that the decreased pattern of rCBF in adult-onset PKAN is different from that of early-onset cases. Yamashita et al. reported that ^{99m}Tc-ECD SPECT of an adult-onset PKAN patient showed hypoperfusion in the bilateral globus pallidus, the left side of the temporal lobe, and the brain stem [13]. Because they did not describe whether the decreased rCBF in the lesions was evaluated with voxel-by-voxel analysis or whether the changes were statistically significant, we cannot make a simple comparison between our cases and their case. Examination of further cases is necessary to confirm whether a decrease in rCBF in the frontoparietal lobes is common in adult-onset PKAN patients. In patients with juvenile and adult-onset HSS, which is probably the same disease as PKAN, α-synuclein-positive Lewy bodies were observed in diseased brain [32,33]. Because cardiac uptake of MIBG is often impaired in Parkinson disease and dementia with Lewy bodies [34], we conducted ^{123}I-MIBG myocardial scintigraphy in both patients. Our results showed normal cardiac uptake of MIBG in both cases. Our findings indicated that cardiac sympathetic nerve function was normal in PKAN patients. These brain perfusion SPECT with voxel-by-voxel analyses and MIBG scintigraphy results in adult-onset PKAN patients have not been previously reported.

Pantothenate kinase catalyzes the first and rate-controlling step in the biosynthesis of CoA [35]. A deficiency in pantothenate kinase 2 may cause cysteine accumulation in the globus pallidus, leading to neuronal death from oxidative stress [4]. Although diverse *PANK2*

mutations have been reported as being responsible for PKAN, the detailed mechanisms that cause iron accumulation are still unknown. Moreover, a therapeutic strategy for PKAN has not been established. The analysis of genotype–phenotype correlations and the elucidation of effects of mutations on pantothenate kinase 2 function, expression, and structure are essential for understanding the mechanisms of PKAN.

References

[1] Dooling EC, Schoene WC, Richardson Jr EP. Hallervorden–Spatz syndrome. Arch Neurol 1974 Jan;30(1):70–83.

[2] Gordon N. Pantothenate kinase-associated neurodegeneration (Hallervorden–Spatz syndrome). Eur J Paediatr Neurol 2002;6(5):243–7.

[3] Swaiman KF. Hallervorden–Spatz syndrome. Pediatr Neurol 2001 Aug;25(2):102–8.

[4] Zhou B, Westaway SK, Levinson B, Johnson MA, Gitschier J, Hayflick SJ. A novel pantothenate kinase gene (*PANK2*) is defective in Hallervorden–Spatz syndrome. Nat Genet 2001 Aug;28(4):345–9.

[5] Hayflick SJ, Westaway SK, Levinson B, Zhou B, Johnson MA, Ching KH, et al. Genetic, clinical, and radiographic delineation of Hallervorden–Spatz syndrome. N Engl J Med 2003 Jan 2;348(1):33–40.

[6] Thomas M, Hayflick SJ, Jankovic J. Clinical heterogeneity of neurodegeneration with brain iron accumulation (Hallervorden–Spatz syndrome) and pantothenate kinase-associated neurodegeneration. Mov Disord 2004 Jan;19(1):36–42.

[7] Zhang YH, Tang BS, Zhao AL, Xia K, Long ZG, Guo JF, et al. Novel compound heterozygous mutations in the *PANK2* gene in a Chinese patient with atypical pantothenate kinase-associated neurodegeneration. Mov Disord 2005 Jul;20(7):819–21.

[8] Ching KH, Westaway SK, Gitschier J, Higgins JJ, Hayflick SJ. HARP syndrome is allelic with pantothenate kinase-associated neurodegeneration. Neurology 2002 Jun 11;58(11):1673–4.

[9] Saleheen D, Ali T, Aly Z, Khealani B, Frossard PM. Novel mutation in the *PANK2* gene leads to pantothenate kinase-associated neurodegeneration in a Pakistani family. Pediatr Neurol 2007 Oct;37(4):296–8.

[10] Kazek B, Jamroz E, Gencik M, Jezela Stanek A, Marszal E, Wojaczynska-Stanek K. A novel *PANK2* gene mutation: clinical and molecular characteristics of patients short communication. J Child Neurol 2007 Nov;22(11):1256–9.

[11] Rump P, Lemmink HH, Verschuuren-Bemelmans CC, Grootscholten PM, Fock JM, Hayflick SJ, et al. A novel 3-bp deletion in the *PANK2* gene of Dutch patients with pantothenate kinase-associated neurodegeneration: evidence for a founder effect. Neurogenetics 2005 Dec;6(4):201–7.

[12] Chan KY, Lam CW, Lee LP, Tong SF, Yuen YP. Pantothenate kinase-associated neurodegeneration in two Chinese children: identification of a novel *PANK2* gene mutation. Hong Kong Med J 2008 Feb;14(1):70–3.

[13] Yamashita S, Maeda Y, Ohmori H, Uchida Y, Hirano T, Yonemura K, et al. Pantothenate kinase-associated neurodegeneration initially presenting as postural tremor alone in a Japanese family with homozygous N245S substitutions in the pantothenate kinase gene. J Neurol Sci 2004 Oct 15;225(1–2):129–33.

[14] Vasconcelos OM, Harter DH, Duffy C, McDonough B, Seidman JG, Seidman CE, et al. Adult Hallervorden–Spatz syndrome simulating amyotrophic lateral sclerosis. Muscle Nerve 2003 Jul;28(1):118–22.

[15] Houlden H, Lincoln S, Farrer M, Cleland PG, Hardy J, Orrell RW. Compound heterozygous *PANK2* mutations confirm HARP and Hallervorden–Spatz syndromes are allelic. Neurology 2003 Nov 25;61(10):1423–6.

[16] Pellecchia MT, Valente EM, Cif L, Salvi S, Albanese A, Scarano V, et al. The diverse phenotype and genotype of pantothenate kinase-associated neurodegeneration. Neurology 2005 May 24;64(10):1810–2.

[17] Antonini A, Goldwurm S, Benti R, Prokisch H, Ebhardt M, Cilia R, et al. Genetic, clinical, and imaging characterization of one patient with late-onset, slowly progressive, pantothenate kinase-associated neurodegeneration. Mov Disord 2006 Mar;21(3):417–8.

[18] Chung SJ, Lee JH, Lee MC, Yoo HW, Kim GH. Focal hand dystonia in a patient with *PANK2* mutation. Mov Disord 2008 Feb 15;23(3):466–8.

[19] Baumeister FA, Auer DP, Hortnagel K, Freisinger P, Meitinger T. The eye-of-the-tiger sign is not a reliable disease marker for Hallervorden–Spatz syndrome. Neuropediatrics 2005 Jun;36(3):221–2.

[20] Wu YR, Chen CM, Chao CY, Lyu RK, Lee-Chen GJ. Pantothenate kinase-associated neurodegeneration in two Taiwanese siblings: identification of a novel *PANK2* gene mutation. Mov Disord 2009 Apr 30;24(6):940–1.

[21] Dubois B, Slachevsky A, Litvan I, Pillon B. The FAB, a Frontal Assessment Battery at bedside. Neurology 2000 Dec 12;55(11):1621–6.

[22] Hashimoto R, Meguro K, Lee E, Kasai M, Ishii H, Yamaguchi S. Effect of age and education on the Trail Making Test and determination of normative data for Japanese elderly people: the Tajiri Project. Psychiatry Clin Neurosci 2006 Aug;60(4):422–8.

[23] Nelson HE. A modified card sorting test sensitive to frontal lobe defects. Cortex 1976 Dec;12(4):313–24.

[24] Hayflick SJ, Hartman M, Coryell J, Gitschier J, Rowley H. Brain MRI in neurodegeneration with brain iron accumulation with and without *PANK2* mutations. AJNR Am J Neuroradiol 2006 Jun-Jul;27(6):1230–3.

[25] Waragai M, Yamada T, Matsuda H. Evaluation of brain perfusion SPECT using an easy Z-score imaging system (eZIS) as an adjunct to early-diagnosis of neurodegenerative diseases. J Neurol Sci 2007 Sep 15;260(1–2):57–64.

[26] Matsuda H, Mizumura S, Nagao T, Ota T, Iizuka T, Nemoto K, et al. Automated discrimination between very early Alzheimer disease and controls using an easy Z-score imaging system for multicenter brain perfusion single-photon emission tomography. AJNR Am J Neuroradiol 2007 Apr;28(4):731–6.

[27] Ashendorf L, Jefferson AL, O'Connor MK, Chaisson C, Green RC, Stern RA. Trail Making Test errors in normal aging, mild cognitive impairment, and dementia. Arch Clin Neuropsychol 2008 Mar;23(2):129–37.

[28] Abe M, Suzuki K, Okada K, Miura R, Fujii T, Etsurou M, et al. [Normative data on tests for frontal lobe functions: Trail Making Test, Verbal fluency, Wisconsin Card Sorting Test (Keio version)]. No To Shinkei. 2004 Jul; 56(7):567–74.

[29] Kanazawa A, Mizuno Y, Narabayashi H. Executive function in Parkinson's disease. Rinsho Shinkeigaku 2001 Apr–May;41(4–5):167–72.

[30] Kobor J, Javaid A, Omojola MF. Cerebellar hypoperfusion in infantile neuroaxonal dystrophy. Pediatr Neurol 2005 Feb;32(2):137–9.

[31] Castelnau P, Zilbovicius M, Ribeiro MJ, Hertz-Pannier L, Ogier H, Evrard P. Striatal and pontocerebellar hypoperfusion in Hallervorden–Spatz syndrome. Pediatr Neurol 2001 Aug;25(2):170–4.

[32] Arawaka S, Saito Y, Murayama S, Mori H. Lewy body in neurodegeneration with brain iron accumulation type 1 is immunoreactive for alpha-synuclein. Neurology 1998 Sep;51(3):887–9.

[33] Wakabayashi K, Yoshimoto M, Fukushima T, Koide R, Horikawa Y, Morita T, et al. Widespread occurrence of alpha-synuclein/NACP-immunoreactive neuronal inclusions in juvenile and adult-onset Hallervorden–Spatz disease with Lewy bodies. Neuropathol Appl Neurobiol 1999 Oct;25(5):363–8.

[34] Nakajima K, Yoshita M, Matsuo S, Taki J, Kinuya S. Iodine-123-MIBG sympathetic imaging in Lewy-body diseases and related movement disorders. Q J Nucl Med Mol Imaging 2008 Dec;52(4):378–87.

[35] Rock CO, Calder RB, Karim MA, Jackowski S. Pantothenate kinase regulation of the intracellular concentration of coenzyme A. J Biol Chem 2000 Jan 14;275(2):1377–83.

RESEARCH LETTER

AMERICAN JOURNAL OF medical genetics

De Novo Deletion of 1q24.3-q31.2 in a Patient With Severe Growth Retardation

Akira Nishimura,[1] Yoko Hiraki,[1,2] Hiroko Shimoda,[3] Gen Nishimura,[4] Hiromi Tadaki,[1] Yoshinori Tsurusaki,[1] Noriko Miyake,[1] Hirotomo Saitsu,[1] and Naomichi Matsumoto[1]*

[1]Department of Human Genetics, Yokohama City University Graduate School of Medicine, Yokohama, Japan

[2]Hiroshima Municipal Center for Child Health and Development, Hiroshima, Japan

[3]Department of Pediatrics, National Hospital Organization, Higashi-Hiroshima Medical Center, Higashi-Hiroshima, Japan

[4]Department of Radiology, Tokyo Metropolitan Kiyose Children's Hospital, Kiyose, Japan

Received 9 November 2009; Accepted 28 January 2010

How to Cite this Article:
Nishimura A, Hiraki Y, Shimoda H, Nishimura G, Tadaki H, Tsurusaki Y, Miyake N, Saitsu H, Matsumoto N. 2010. De novo deletion of 1q24.3-q31.2 in a patient with severe growth retardation.
Am J Med Genet Part A 152A:1322–1325.

TO THE EDITOR:

Interstitial 1q deletions have been classified into three groups: proximal deletion (1q21-22q25), intermediate (1q24-25q32), and distal (1q42-43qter) [Taysi et al., 1982]. To our knowledge, only seven deletions have been characterized by molecular methods [Franco et al., 1991; Takano et al., 1997; Melis et al., 1998; Pallotta et al., 2001; Hoglund et al., 2003; Chaabouni et al., 2006; Descartes et al., 2008]. We report on a patient with 1q24.3-q31.2 deletion, which was thoroughly analyzed by high density SNP array as well as junctional cloning.

The propositus is a $3\frac{1}{3}$-year-old boy. He was born at 35 weeks of gestation by cesarean due to fetal distress of nonconsanguineous 39-year-old mother and 37-year-old father. Intrauterine growth retardation was suspected at 27 weeks of gestation. Birth length was 36 cm (−3.7 SD), weight 1,324 g (−3.8 SD), and head circumference (OFC) 29 cm (−1.5 SD). At age of $3\frac{1}{3}$ years, his length is 65 cm (−8.5 SD), weight 5,890 g (−4.5 SD), and OFC 41.6 cm (−5.5 SD), indicating obvious pre- and postnatal growth retardation. Multiple anomalies were recognized: prominent forehead, sparse, and fine hair, decreased expression of the face, deep-set eyes, prominent cupid bow, left ptosis, left exotropia and strabismus, short philtrum, downturned corners of the mouth, high-arched palate, low-set ears, small hands and feet, bilateral simian creases, bilateral fifth clinodactyly, bilateral inguinal hernia, cryptorchidism, and small penis.

Radiographs showed the following findings. The upper thorax is asymmetrically narrow as a result of unequally short upper ribs. The ribs were 12 in number. Incomplete congruence of the hip joints was noted together with deep acetabular angles. The distal ulnae were relatively elongated, and they were somewhat displaced ulnarly. The distal radial articular surfaces were unusually tilted radially. In the hands, the middle phalanges, particularly of the index and little fingers, were short and bullet-shaped. The terminal tufts of the distal phalanges, particularly of the second, were somewhat hypoplastic. The fifth metacarpals were broad and short. Carpal ossification was significantly delayed. In feet, he middle and distal phanageal ossification was incomplete.

Bilateral low-tone hearing loss (mixed-type) and otitis media were observed. He was barely able to walk at 3 years. Head magnetic resonance imaging showed no abnormality. Serum TSH, fT3, and fT4 were normal. IGF-1 and IGFBP-3 were low [4.0 ng/ml (normal range: 11–172 ng/ml) and 0.34 μg/ml (normal range: 1.02–2.50 μg/ml), respectively] and GH stimulation test by clonidine and L-DOPA indicated GH deficiency [0.76 ng/ml and 0.49 ng/ml at maximum, respectively (pathological range: <6 ng/ml)]. Serum antithrombin III (AT III) was also at a low level [13.7 mg/dl (normal range: 23.6–33.5 mg/dl), 48% in activity (normal range: 79–121%)].

GTG-binding chromosome analysis of the patient's blood lymphocytes demonstrated 46,XY,del(1)(q23q25),t(4;11)(q31.3;q21) (Fig. 1a). Parental karyotype was all normal. Affymetrix GeneChip

Grant sponsor: Ministry of Health, Labour and Welfare; Grant sponsor: Ministry of Education, Culture, Sports, Science and Technology of Japan.
*Correspondence to:
Naomichi Matsumoto, Department of Human Genetics, Yokohama City University Graduate School of Medicine, Fukuura 3-9, Kanazawa-ku, Yokohama 236-0004, Japan. E-mail: naomat@yokohama-cu.ac.jp
Published online 13 April 2010 in Wiley InterScience (www.interscience.wiley.com)
DOI 10.1002/ajmg.a.33371

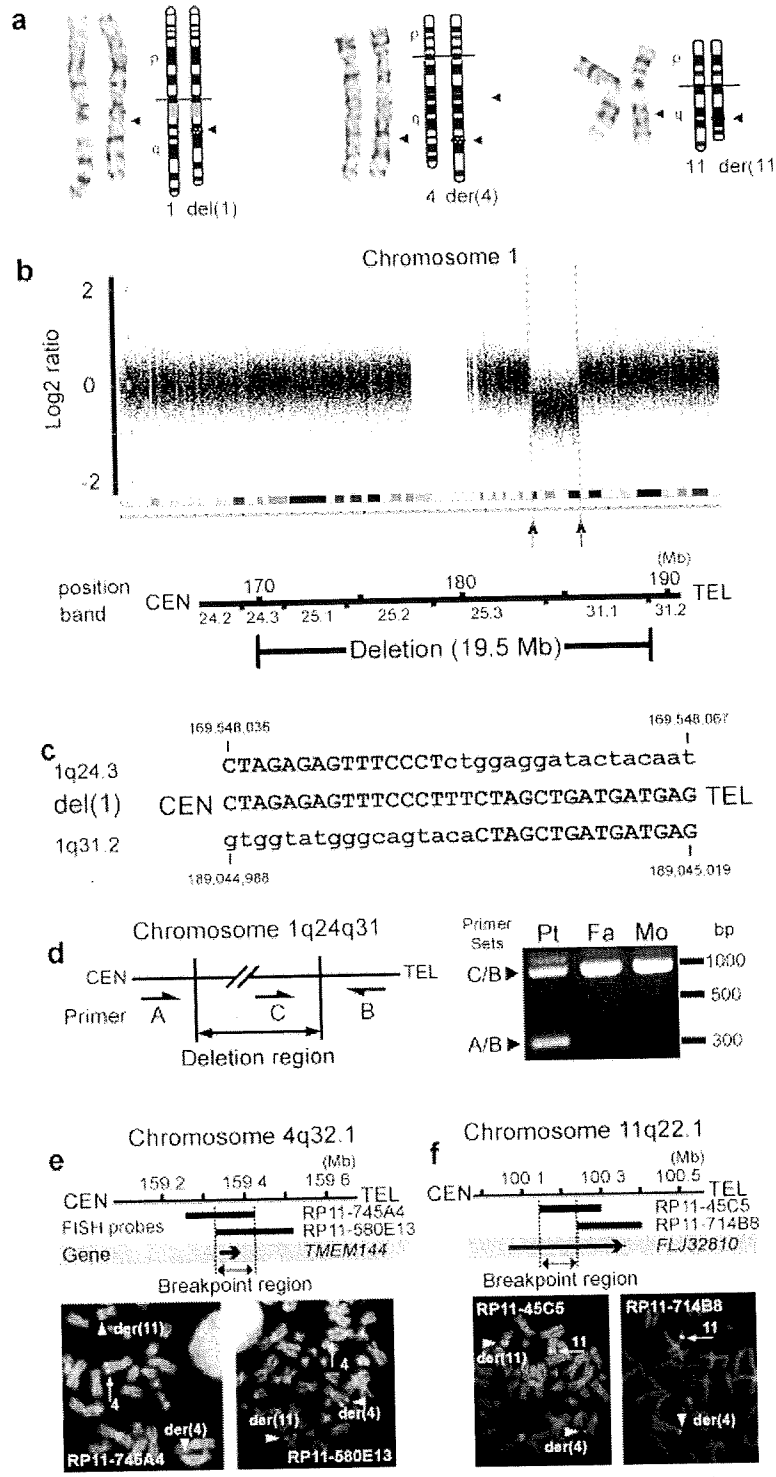

FIG. 1. Analysis of 1q24.2-q31.2 deletion and t(4;11). a: Partial karyotype of chromosomes 1,4, and 11 in the patient. b: High-resolution SNP array revealed the 19.5-Mb deletion. *Y* and *X* axes indicate probe signal intensity (log_2 ratio) and probe potion in chromosome 1, respectively, in the upper, ideogram of chromosome 1 in the middle, and location of the deletion in the lower. c: Deletion junction sequence. Upper and lower sequences are normal ones around at proximal (1q24.3) and distal (1q31.2) deletion breakpoints, respectively. Middle shows deletion junction in the patient. Gray shadow shows matched sequences. d: Primer positions of PCR specific to normal (C/B) and deleted (A/B) chromosomes 1 (left) and results of PCR in trio's DNA. Deletion occurred de novo. Pt: patient, Fa: father, Mo: mother. e: 4q32.1 breakpoint analysis. RP11-745A4 (left) and RP11-580E13 (right) spanned the 4q32.1breakpoint. f: 11q22.1 breakpoint analysis. RP11-45C5 (left) spanned the 11q22.1 breakpoint, and RP11-714B8 (right) was mapped distal to the breakpoint. Translocation region was between dotted vertical lines in (e) and (f).

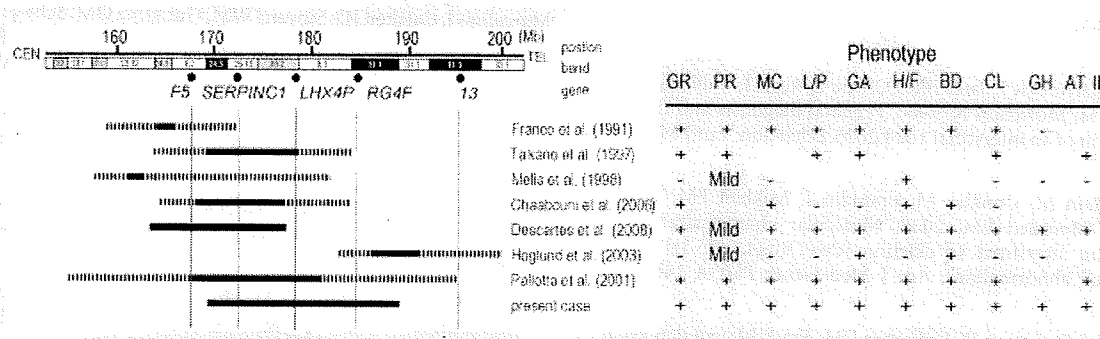

FIG. 2. Molecularly defined 1q interstitial deletions and their clinical phenotypes. From upper to lower, chromosomal bands of 1q reported deletions, genes, and reported deletions were shown. Solid and dashed horizontal bars are confirmed deletion and possible (unconfirmed) deletion, respectively. Phenotypes of each deletion are listed up in right gray box. GR, growth retardation; PR, psychomotor retardation; MC, microcephaly; L/P, lip/palate anomalies; GA, genital abnormalities; H/F, small hands/feet; BD, brachydactyly; CL, fifth finger clinodactyly; GH, reduced of growth hormone; AT III, ATIII deficiency; +, positive; −, negative.

Human SNP array 6.0 (Affymetrix, Santa Clara, CA) was used for further analysis. Genomic DNA was isolated from peripheral blood lymphocytes of the patient using QuickGene-610L (Fujifilm, Tokyo, Japan). DNA (250 ng) were digested with *Nsp*I and *Sty*I, ligated with adaptor, PCR-amplified, purified by using magnetic beads, fragmented, labeled, and hybridized to the array. Data analysis was done by Genotyping Console 3.0.1 (Affymetrix). SNP array clearly demonstrated 1q24.3-q31.2 deletion (Fig. 1b), but could not reveal any other fortuitous copy number changes associated with t(4;11). The deletion junction was successfully amplified by PCR using primers (F: 5′-CCTTCTCCCTAGGCCAGCTTCATTC-3′, R: 5′-ATGAGCAGCTGGGAAGGCTTAATTG-3′) and sequenced. The deleted region spanned from 169,548,050–189,045,005 (19,496,955 bp according to the UCSC genome browser, 2006 Mar version, hg18) with two nucleotides insertion of unknown origin (TT) (Fig. 1c). Primers designed to amplify normal chromosomal fragment (with primers C and B) and abnormal fragment (with primers A and B) showed the deletion occurred de novo (Fig. 1d) (primer information is available on request). FISH analysis of chromosomes of the patient and his parents using two BACs mapped within the deletion (RP11-81H19 and RP11-463J7) and two other BACs adjacent to the deletion (but outside) (RP11-79E17 and RP11-184F4) confirmed the de novo deletion in one of chromosomes (data not shown). Microsatellite analysis of the trio's DNA using *D1S218* and *D1S238* revealed the deleted chromosome was of paternal origin (data not shown).

The t(4;11) was analyzed by BAC-FISH. RP11-745A4 and RP11-580E13 spanned the 4q32.1 breakpoint (Fig. 1e). Overlapped region between the two BACs was localized to the position of 159,325,668–159,422,337 (chr 4) according to the UCSC genome browser. Regarding the 11q21 breakpoint, RP11-45C5 spanned the breakpoint while RP11-714B8 was mapped distal to the breakpoint (Fig. 1f). These suggest the 11q breakpoint was positioned to the ~100-kb region of 100,145,397–100,233,747 (chr 11).

Although seven cases of 1q interstitial deletions defined with molecular techniques have been reported, resolution of the mappings was low [Franco et al., 1991; Takano et al., 1997; Melis et al., 1998; Pallotta et al., 2001; Hoglund et al., 2003; Chaabouni et al., 2006; Descartes et al., 2008]. We could precisely map the deletion and clone the deletion junction for the first time.

Phenotype–genotype correlations of the eight above cases provides interesting information (Fig. 2). Growth retardation may be associated with heterozygous *LHX4* (LIM homeobox gene 4) deletion. LHX4 plays an important role in pituitary development involving GH secretion [Machinis et al., 2001]. As dominant and fully penetrant effects of a splice mutation of *LHX4* was clearly shown [Machinis et al., 2001], the negative effect of its heterozygous deletion on GH secretion is obvious. Regarding psychomotor retardation, no particular genes within deletions are found to be related, but the impact of a large deletion like our case may not be small. It is clear that *SERPINC1* (serpin peptidase inhibitor, clade C member 1 gene) deletion results in AT III deficiency (OMIM +107300). Biallelic *PRG4* (Proteoglycan 4 gene) mutations causes camptodactyly-arthropathy-coxa vara-pericarditis syndrome [Marcelino et al., 1999]. Heterozygous *PRG4* deletion might be partially related to some skeletal abnormalities. It should be noted that t(4;11) may alter expression of genes, *TMEM144* at 4q32.1 and *FLJ32810* at 11q21, though their precise functions are yet unknown.

In conclusion, we clone the 1q24.3-q31.2 deletion junction and precisely mapped the balanced translocation of t(4;11). Pathological chromosomal changes should be investigated at the nucleotide level, then gene dosage effects associated with chromosomal changes may help in explaining complex disease phenotypes.

ACKNOWLEDGMENTS

We would like to thank the patient and his parents for their participation in this study. This work is supported by Grant-in Aid for Japan Society for the Promotion of Science (JSPS) Fellow (A.N.), Research Grants from the Ministry of Health, Labour and Welfare (N.M.), Grant-in-Aid for Scientific Research on Priority Areas (Research on Pathomechanisms of Brain disorder) from the Ministry of Education, Culture, Sports, Science and Technology of Japan (N.M.), and Grant-in-Aid for Scientific Research from JSPS (N.M.).

REFERENCES

Chaabouni M, Martinovic J, Sanlaville D, Attie-Bittach T, Caillat S, Turleau C, Vekemans M, Morichon N. 2006. Prenatal diagnosis and molecular characterization of an interstitial 1q24.2q25.2 deletion. Eur J Med Genet 49:487–493.

Descartes M, Hain JZ, Conklin M, Franklin J, Mikhail FM, Lachman RS, Nolet S, Messiaen LM. 2008. Molecular characterization of a patient with an interstitial 1q deletion [del(1)(q24.1q25.3)] and distinctive skeletal abnormalities. Am J Med Genet Part A 146A:2937–2943.

Franco B, Lai LW, Patterson D, Ledbetter DH, Trask BJ, van den Engh G, Iannaccone S, Frances S, Patel PI, Lupski JR. 1991. Molecular characterization of a patient with del(1)(q23-q25). Hum Genet 87:269–277.

Hoglund P, Jalkanen R, Marttinen E, Alitalo T. 2003. Interstitial 1q25.3-q31.3 deletion in a boy with mild manifestations. Am J Med Genet Part A 123A:290–295.

Machinis K, Pantel J, Netchine I, Leger J, Camand OJ, Sobrier ML, Dastot-Le Moal F, Duquesnoy P, Abitbol M, Czernichow P, Amselem S. 2001. Syndromic short stature in patients with a germline mutation in the LIM homeobox LHX4. Am J Hum Genet 69:961–968.

Marcelino J, Carpten JD, Suwairi WM, Gutierrez OM, Schwartz S, Robbins C, Sood R, Makalowska I, Baxevanis A, Johnstone B, Laxer RM, Zemel L, Kim CA, Herd JK, Ihle J, Williams C, Johnson M, Raman V, Alonso LG, Brunoni D, Gerstein A, Papadopoulos N, Bahabri SA, Trent JM, Warman ML. 1999. CACP, encoding a secreted proteoglycan, is mutated in camptodactyly-arthropathy-coxa vara-pericarditis syndrome. Nat Genet 23:319–322.

Melis D, Perone L, Sperandeo MP, Sabbatino MS, Tuzzi MR, Romano A, Parenti G, Andria G. 1998. Mild phenotype associated with an interstitial deletion of the long arm of chromosome 1. J Med Genet 35:1047–1049.

Pallotta R, Dalpra L, Miozzo M, Ehresmann T, Fusilli P. 2001. A patient defines the interstitial 1q deletion syndrome characterized by antithrombin III deficiency. Am J Med Genet 104:282–286.

Takano T, Yamanouchi Y, Mori Y, Kudo S, Nakayama T, Sugiura M, Hashira S, Abe T. 1997. Interstitial deletion of chromosome 1q [del(1)(q24q25.3)] identified by fluorescence in situ hybridization and gene dosage analysis of apolipoprotein A-II, coagulation factor V, and antithrombin III. Am J Med Genet 68:207–210.

Taysi K, Sekhon GS, Hillman RE. 1982. A new syndrome of proximal deletion of the long arm of chromosome 1: 1q21-23 leads to 1q25. Am J Med Genet 13:423–430.

Neurogenetics
DOI 10.1007/s10048-010-0245-6

ORIGINAL ARTICLE

Analysis of an insertion mutation in a cohort of 94 patients with spinocerebellar ataxia type 31 from Nagano, Japan

Haruya Sakai · Kunihiro Yoshida · Yusaku Shimizu · Hiroshi Morita · Shu-ichi Ikeda · Naomichi Matsumoto

Received: 11 February 2010 / Accepted: 13 April 2010

Abstract Spinocerebellar ataxia type 31 (SCA31) is a recently defined subtype of autosomal dominant cerebellar ataxia (ADCA) characterized by adult-onset, pure cerebellar ataxia. The C/T substitution in the 5′-untranslated region of the *puratrophin-1* gene (*PLEKHG4*) or a disease-specific haplotype within the 900-kb SCA31 critical region just upstream of *PLEKHG4* has been used for the diagnosis of SCA31. Very recently, a disease-specific insertion containing penta-nucleotide $(TGGAA)_n$ repeats has been found in this critical region in SCA31 patients. SCA31 was highly prevalent in Nagano, Japan, where SCA31 accounts for approximately 42% of ADCA families. We screened the insertion in 94 SCA31 patients from 71 families in Nagano. All patients had a 2.6- to 3.7-kb insertion. The size of the insertion was inversely correlated with the age at onset but not associated with the progression rate after onset. $(TAGAA)_n$ repeats at the 5′-end of the insertion were variable in number, ranging from 0 (without TAGAA sequence) to 4. The number of $(TAGAA)_n$ repeats was inversely correlated to the total size of the insertion. The number of $(TAGAA)_n$ repeats was comparatively uniform within patients from the three endemic foci in Nagano. Only one patient, heterozygous for the C/T substitution in *PLEKHG4*, had the insertions in both alleles; they were approximately 3.0 and 4.3 kb in size. Sequencing and Southern hybridization using biotin-labeled $(TGGAA)_5$ probe strongly indicated that the 3.0-kb insertion, but not the 4.3-kb insertion, contained $(TGGAA)_n$ stretch. We also found that 3 of 405 control individuals (0.7%) had the insertions from 1.0 to 3.5 kb in length. They were negative for the C/T substitution in *PLEKHG4*, and neither of the insertions contained $(TGGAA)_n$ stretch at their 5′-end by sequencing. The insertions in normal controls were clearly detected by Southern hybridization using $(TAAAA)_5$ probe, while they were not labeled with $(TGGAA)_5$ or $(TAGAA)_5$ probe. These data indicate that control alleles very rarely have a nonpathogenic large insertion in the SCA31 critical region and that not only the presence of the insertion but also its size is not sufficient evidence for a disease-causing allele. We approve of the view that $(TGGAA)_n$ repeats in the insertion are indeed related to the pathogenesis of SCA31, but it remains undetermined whether a large insertion lacking $(TGGAA)_n$ is nonpathogenic.

Keywords SCA31 · 16q-ADCA · Puratrophin-1 · Penta-nucleotide repeats · Insertion

Haruya Sakai and Kunihiro Yoshida equally contributed to this work.

Disclosure The authors report no conflicts of interest.

H. Sakai · N. Matsumoto
Department of Human Genetics, Yokohama City University Graduate School of Medicine,
3-9 Fukuura, Kanazawa-ku,
Yokohama 236-0004, Japan

K. Yoshida (✉) · H. Morita · S.-i. Ikeda
Department of Medicine (Neurology and Rheumatology), Shinshu University School of Medicine,
3-1-1 Asahi,
Matsumoto 390-8621, Japan
e-mail: kyoshida@shinshu-u.ac.jp

Y. Shimizu
Department of Neurology, Ina Central Hospital,
1313-1 Ina,
Ina 396-8555, Japan

Published online: 28 April 2010

Introduction

Spinocerebellar ataxia type 31 (SCA31), formerly known as 16q22.1-linked autosomal dominant cerebellar ataxia (16q-

ADCA), is a recently established subtype of ADCA characterized by adult-onset, pure cerebellar ataxia [1–6]. SCA31 accounts for 8–17% of ADCA families and is the third most predominant ADCA subtype after SCA6 and MJD/SCA3 in Japan [7–11]. A single nucleotide substitution (–16C>T) in the 5′-untranslated region (UTR) of the gene encoding *puratrophin-1* (*PLEKHG4*) has been shown to be a disease-specific marker for 16q-ADCA [4, 5]. However, this specific substitution has been found exclusively in the Japanese population [12]; thus, it is still unclear whether SCA31 exists in countries other than Japan.

Two patients with SCA31 have been found not to carry this substitution in *PLEKHG4* [5, 13], indicating that it is not a disease-causing mutation for SCA31. Thereafter, Amino et al. [5] narrowed the SCA31 critical region to 900 kb between rs11640843 (SNP04) and *PLEKHG4* by fine single nucleotide polymorphism (SNP) typing. Sato et al. [6] identified an inserted sequence in this region, which was confirmed in all SCA31 patients, without exception. The insertion consists of complex penta-nucleotide repeats containing $(TGGAA)_n$, and the size of the insertion is variable, ranging from 2.5 to 3.8 kb in length, among patients [6].

We have shown that SCA31 is the most predominant subtype of ADCA in Nagano, which is located in the central, mountainous district of the main island of Japan [13–15], see Fig. 2]. To date, we have analyzed 168 ADCA families from Nagano and diagnosed 71 families (42%) with SCA31. Thus, the frequency of SCA31 in Nagano is much higher than in other areas of Japan [7–11]. We have found that SCA31 families are highly prevalent in particular areas of Nagano, named as Kiso, Ina, and Saku [13–15], see Fig. 2]. The ratio of SCA31 families to total ADCA families in these areas was 14/16 (88%, Kiso area), 12/18 (67%, Ina area), and 17/25 (68%, Saku area).

Here, we have screened an insertion mutation for SCA31 in 94 patients from 71 families in Nagano.

Materials and methods

Subjects and clinical evaluation

We recruited 94 patients from 71 families with SCA31, and these families most probably originated from Nagano. The diagnosis of SCA31 was based on the presence of the C/T substitution in *PLEKHG4* (92 patients from 70 families). Two patients (from two families) without the C/T substitution in *PLEKHG4* were also included in this study because they had a disease-specific haplotype in the 900-kb SCA31 critical region [13]. Forty-four of 71 families (62%) originated from the three endemic foci described above. Detailed medical interviews and routine neurological examinations were performed by expert neurologists. Age at onset was determined on the basis of the information provided by the patients or their close relatives. Scales for the assessment and rating of ataxia (SARA) were used for the assessment of cerebellar ataxia. To minimize the interrater variability, SARA was performed by either of two expert neurologists (KY and YS) for 57 patients (67 times).

This research protocol was approved independently by the Ethical Committee of Shinshu University School of Medicine and by the Committee for Ethical Issues at Yokohama City University Graduate School of Medicine.

Molecular analysis

The insertion sequence was amplified by PCR according to the methods described by Sato et al. [6]. PCR products were purified using a PCR purification kit (QIAGEN), digested with *Hae*III, and then separated on a 0.8% agarose gel (25 V, 15 h). The size of the *Hae*III fragment containing the insertion was calculated with a DNA size marker simultaneously electrophoresed as a reference. *Hae*III-undigested PCR products were separated in a 0.8% low-melting agarose gel, and fragments of approximately 3.0 kb were cut out and extracted using a QIA quick® Gel Extraction Kit (QIAGEN). They were then directly sequenced by a standard protocol using BigDye terminator (Applied Biosystems, Foster City, CA) on an ABI PRISM 3100 Genetic analyzer or an ABI PRISM 3500xL Genetic analyzer (Applied Biosystems). *Hae*III-undigested PCR products were also separated in a 1% agarose gel, blotted to a nylon membrane (Hybond^{TM}- N^{+}, Amersham International plc, Buckinghamshire, UK) using 10× SSC, and subjected to Southern hybridization using biotin-labeled $(TGGAA)_5$, $(TAGAA)_5$, or $(TAAAA)_5$ as a probe. Detection was done with BrightStar^{TM} BioDetect^{TM} Nonisotopic Detection Kit (Ambion Inc., Austin, TX) according to the manufacturer's instructions.

Statistics

The relationship between the size of the insert and the age at onset was analyzed using Spearman's correlation coefficient by rank test. Regression analysis for SARA data was also performed. Analysis of the differences in the insert size among the groups was carried out using analysis of variance and the post hoc test of Scheffé. The level of significance was set at $p<0.01$.

Results

All of the patients recruited in this study had an insertion ranging from 2.6 to 3.7 kb in length. Direct sequencing confirmed that the insertion contained $(TGGAA)_n$ stretch in

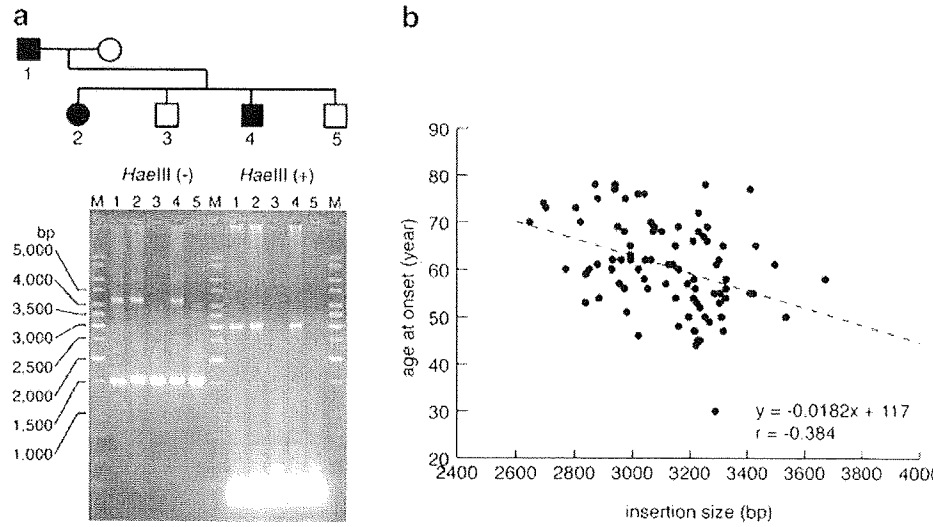

Fig. 1 Correlation between the insertion size and age at onset (n=89). Representative PCR screening for the SCA31 insertion (**a**). Agarose gel electrophoresis of PCR products before and after *Hae*III digestion is shown. *M* GeneRuler^{TM} 1-kb Ladder (Fermentas Life Sciences, Burlington, Canada). The size of the insertion is inversely correlated with the age at onset (**b**). For 5 of 94 patients, age at onset could not be clearly defined by medical interview

all of the patients. The average length of the insertions was approximately 3,130 bp (SD, 199 bp) (n=94). The correlation between the size of the insertion and the age at onset is shown in Fig. 1. The length of the insertion was inversely correlated with the age at onset (n=89). We observed six intergenerational transmission of a disease-causing allele in five families in our cohort. There was no conspicuous expansion of the insertion size.

The average size of the insertion was obviously different between patients from the three endemic foci (Fig. 2a, b). The insertion of patients from Kiso area was significantly shorter in length (2,866±132 bp, n=18) than those from the other two areas (3,263±101 bp, n=27, Ina area; 3,111±109 bp, n=18, Saku area).

We found the number of penta-nucleotide $(TAGAA)_n$ repeats at the 5′-end of the insertion was variable, as well as the subsequent $(TGGAA)_n$ repeats. The number of $(TAGAA)_n$ repeats ranged from 0 to 4 (Fig. 3); the most predominant number was 1 (50/94, 53%), followed by 2 (20/94, 21%), 3 (14/94, 15%), and 4 (8/94, 9%). There were two patients without (TAGAA) sequence just upstream of $(TGGAA)_n$ repeats. The number of $(TAGAA)_n$ repeats, if present, was inversely correlated with the size of the insertion (Fig. 4). The repeat size of $(TAGAA)_n$ was comparatively uniform within the endemic foci. Seventeen of 18 patients (94%) in Kiso area had three or four $(TAGAA)_n$ repeats. Twenty-five of 27 (93%) in Ina area had one repeat, and all 18 patients (100%) in Saku area had one or two repeats. Two patients without (TAGAA) sequence originated from areas outside the three endemic foci. We had 12 families, in which more than two affected members were recruited in this cohort. Intrafamilial variation in $(TAGAA)_n$ repeat number was observed only in one family (family ID 166); the sister had four

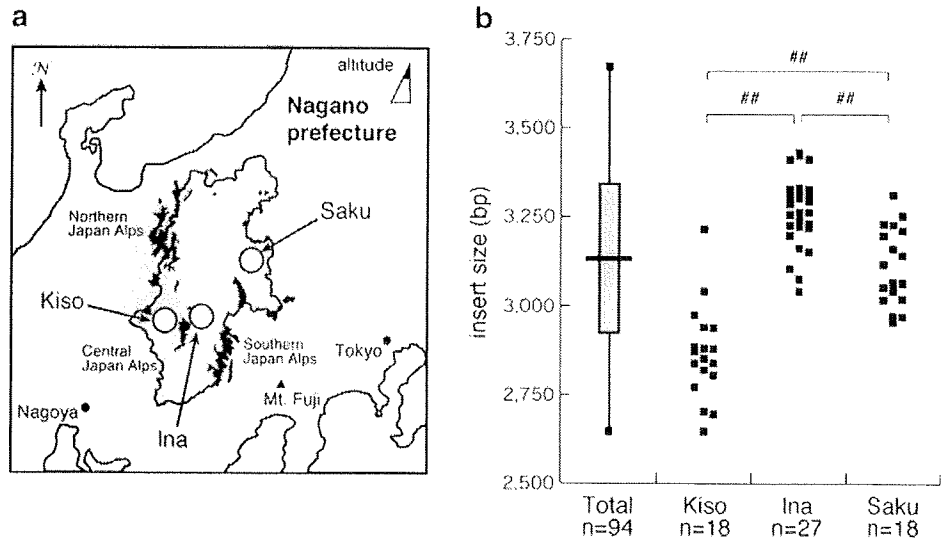

Fig. 2 Distribution of the insertion size in endemic foci in Nagano. The location of the three endemic foci (Kiso, Ina, and Saku) in Nagano prefecture is indicated (**a**). The distribution of the size of insertions in the three endemic foci is shown (**b**). The distribution (*vertical bar*), the average size (*horizontal bar*), and the standard deviation of the size of insertion (*shaded square*) in all the patients (n=94) are shown in left. $^{\#\#}p<0.01$

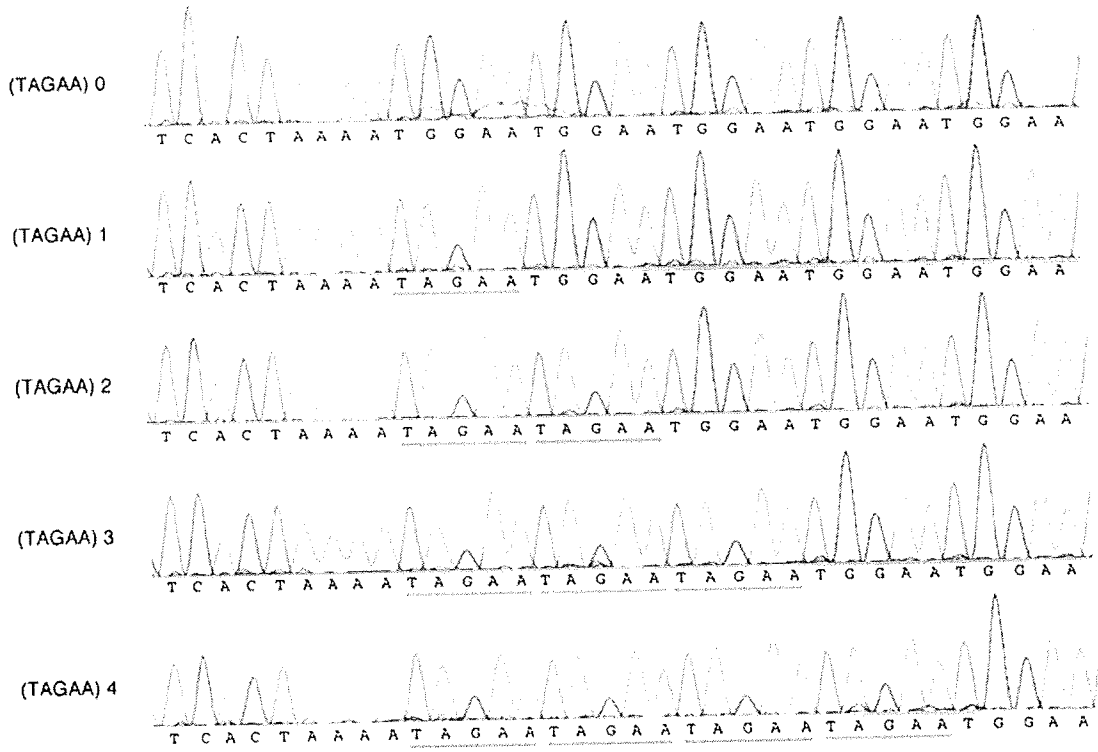

Fig. 3 Sequence of the 5'-end of the insertion. The number of $(TAGAA)_n$ repeats (*underlined in red*) is variable, ranging from 0 to 4

$(TAGAA)_n$ repeats and her younger brother had three, but the number of $(TAGAA)_n$ repeats was consistent among the family members in the other 11 families.

In our cohort, 93 patients were heterozygous for the insertion, but only one patient aged 87 (patient ID 254) carried the insertions in both alleles (Fig. 5). This patient originated from one of three endemic foci, Kiso area, and developed cerebellar ataxia at age 76. He was still able to walk with a cane, and his SARA score was 15.5 at age 87. The size of the insertions was calculated as approximately 3,040 and 4,280 bp. Direct sequencing showed that only the 3.0-kb insertion, but not the 4.3-kb insertion, contained $(TGGAA)_n$ stretch. By Southern hybridization, the 3.0-kb insertion, but not the 4.3-kb insertion, was detected by $(TGGAA)_5$ probe (Fig. 6c). The 4.3-kb insertion was faintly labeled with $(TAGAA)_5$ probe, and the signal intensity was much weaker than the 3.0-kb insertion (Fig. 6d). On the

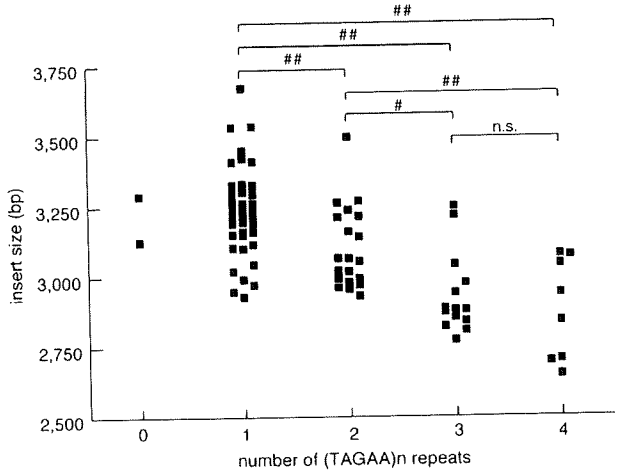

Fig. 4 Correlation between the sizes of $(TAGAA)_n$ repeats preceding $(TGGAA)_n$ repeats and the insertion size. $\#\#p<0.01$; $\#p < 0.05$. n.s. not significant

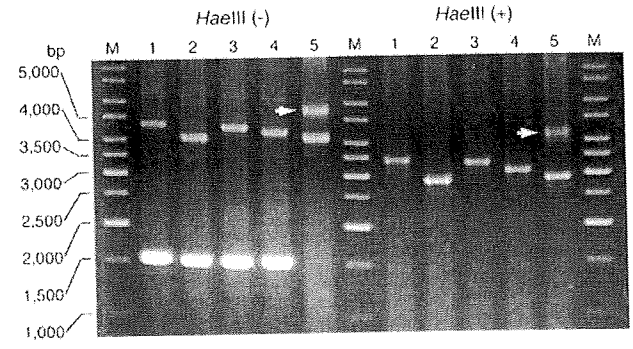

Fig. 5 PCR amplification for the insertion. The patient (ID 256, *lane 5*) had insertions on both alleles, instead of lacking a wild-type 1.5-kb band without the insertion. The 4.3-kb band is indicated by the *arrow*

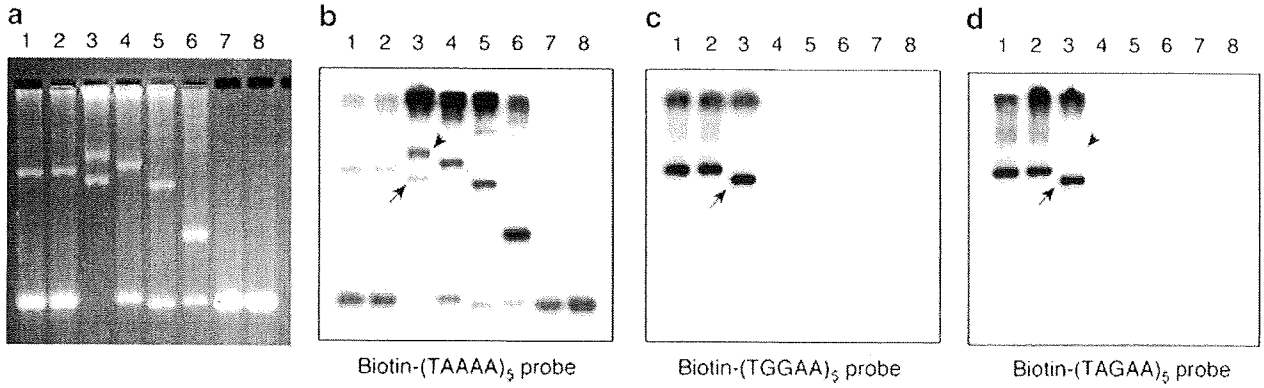

Fig. 6 Southern hybridization for the insertion. *Hae*III-undigested PCR products were separated in a 1% agarose gel, stained with ethidium bromide (**a**), and then blotted to a nylon membrane. The membrane was hybridized with biotin-labeled $(TAAAA)_5$ probe (**b**), $(TGGAA)_5$ probe (**c**), or $(TAGAA)_5$ probe (**d**). The insertions in SCA31 patients (*lanes 1–3*) were clearly detected by $(TGGAA)_5$ or $(TAGAA)_5$ probe (**c** and **d**) . In patient ID 254 (*lane 3*), the 3.0-kb insertion (*arrow*), but not the 4.3-kb insertion (*arrowhead*), was clearly labeled with $(TGGAA)_5$ probe (**c**). In contrast, the 4.3-kb insertion (*arrowhead*), as well as the insertions in normal controls (*lanes 4–6*), was more intensively labeled with $(TAAAA)_5$ probe than the insertions in SCA31 patients (**b**). The 1.5-kb fragments derived from a normal allele were visualized by $(TAAAA)_5$ probe (**b**) because $(TAAAA)_n$ repeats are included in the original genomic sequence. *Lanes 1–3* ,SCA31 patients (*lane 3*, patient ID 254); *lanes 4–6*, control individuals with the insertion (*lane 4*: control 1; *lane 5*: control 2; *lane 6*: control 3 in Table 1); *lanes 7 and 8*, control individuals without the insertion

other hand, the 4.3-kb insertion was more intensively labeled with $(TAAAA)_5$ probe than the 3.0-kb insertion (Fig. 6b).

Furthermore, we found that 3 of 405 healthy control individuals (0.7%) had the insertions (Fig. 6a, Table 1). Neither of the insertions contained $(TGGAA)_n$ stretch at their 5′-end by sequencing. By Southern hybridization, the insertions in control individuals were not detected by $(TGGAA)_5$, or $(TAGAA)_5$ probe (Fig. 6c, d), but were more clearly labeled with $(TAAAA)_5$ probe than the insertions in SCA31 patients (Fig. 6b).

To see the effect of the insertion size on disease progression, we tentatively divided the patients into three groups based on the size of the insertion; groups I (insertion size>3,300 bp, n=11), II (3,000–3,300 bp, n=27), and III (<3,000 bp, n = 17). The correlation between SARA scores and age at examination or duration of illness is shown in Fig. 7. There was no significant difference in the disease progression rate after onset between the groups.

Discussion

In the present study, we confirmed that all of the SCA31 patients in our cohort had the insertions of the penta-nucleotide repeats found by Sato et al. [6]. The insertions ranged from 2.6 to 3.7 kb in length, and contained $(TGGAA)_n$ stretch at their 5′-end, without exception. We also verified that the size of the insertion was inversely correlated to the age at disease onset in our large cohort.

Table 1 The haplotypes of SCA31 patients and control subjects

Polymorphic marker (site on NCBI Build 36.3)	AB473220 (65,049,291)	Complex penta-nucleotide repeat insertion [insertion size] (65,081,803)	AB473217 (65,114,245)	−16C/T *puratrophin-1* (65,871,433)
Reference sequence	G	–	G	C
Frequencies in controls[a]	G 99.2%		G 100%	C 100%
	A 0.8%		C 0.0%	T 0.0%
Homozygous patient[a]	A	5′ TCAC (TGGAA)n (TAAAA TAGAA)n–	C	T
Patient (ID 254)[b]	A	5′ TCAC TAAAA (TAGAA)4 (TGGAA)n – [3,040 bp] 5′ TCAC TAACA (TAAAA)n – [4,280 bp]	G/C	C/T
Control 1[b]	G/A	5′ TCAC TAACA (TAAAA)n – [3,520 bp]	G	C
Control 2[b]	G	5′ (TAAAA)n – [2,540 bp]	G	C
Control 3[b]	G	5′ (TAAAA)n – [1,070 bp]	G	C

[a] Sato et al (2009)

[b] This study

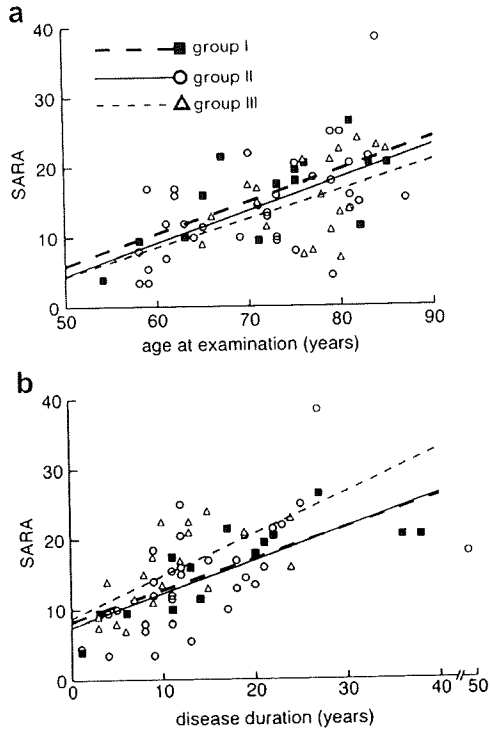

Fig. 7 Correlation between SARA and age at examination (**a**) or duration of disease (**b**) in SCA31 patients. The patients were divided into three groups based on the size of insertion; groups I (insertion size >3,300 bp, *closed square*), II (3,000–3,300 bp, *open circle*), and III (<3,000 bp, *open triangle*). SARA was performed 14 times in 11 patients from group I, 34 times in 29 patients from group II, and 19 times in 17 patients from group III. *Broken*, *solid*, and *dotted lines* indicate linear regression lines for groups I, II, and III, respectively

However, the size of the insertion seemed not to be associated with the disease progression rate after onset.

We found that the penta-nucleotide $(TAGAA)_n$ repeats at the 5′-end of the insertion were variable in number, as were the subsequent $(TGGAA)_n$ repeats. Interestingly, the number of $(TAGAA)_n$ repeats, if present, was inversely correlated with the total size of the insertion. Furthermore, the repeat size of $(TAGAA)_n$ is comparatively uniform within the endemic foci. From the geographical viewpoint, we previously supposed that there were two major foci in the southwest (Ina–Kiso) and east (Saku) areas in Nagano [15], but patients in Ina and Kiso areas are likely to be different from the viewpoint of population genetics because the number of $(TAGAA)_n$ repeats and the size of the insertion were obviously different between the two groups.

In our cohort, only one patient (patient ID 254) was homozygous for the insertion in the SCA31 critical region as determined by PCR analysis (Fig. 5, Table 1). Contrary to our expectation, sequencing showed that only the smaller 3.0-kb insertion had $(TGGAA)_n$ stretch. This was also confirmed by Southern hybridization using biotin-labeled $(TGGAA)_5$ probe. The patient developed gait ataxia at approximately age 76 and showed pure cerebellar ataxia by neurological examination at age 87. His clinical features were typical for SCA31 [7–11, 13, 15]. As his parents died a long time ago, we could not obtain reliable information on his parents or their genomic DNA. It is confusing that he was heterozygous for the C/T substitution in *PLEKHG4* but was homozygous for a disease-specific G/A substitution at AB473220 (Table 1).

Moreover, three control individuals had the insertions ranging from 1.0 to 3.5 kb in length. Sequencing and Southern hybridization indicated that these insertions did not contain $(TGGAA)_n$ or $(TAGAA)_n$ repeats. Information on the family history of cerebellar ataxia was not available for these control individuals because they voluntarily participated in this study as anonymous healthy controls. Neither of them carried the C/T substitution in *PLEKHG4*, but one control individual (control 1 in Table 1) had G/A substitution at AB473220 and a large insertion (3,520 bp) indistinguishable from SCA31 patients. Sato et al. [6] have shown that the insertion in the SCA31 critical region is rarely observed in control individuals but that the insertion in control individuals is shorter in length than SCA31 patients and lacks $(TGGAA)_n$ stretch. At present, however, we do not completely exclude the possibility that the 4.3-kb insertion in patient ID 254 and the 3.5-kb insertion in control 1 have some pathogenic effects, although these insertions are likely to lack $(TGGAA)_n$ stretch.

In summary, our data clearly indicate that not only the presence of the insertion but also the size of the insertion in the SCA31 critical region is insufficient evidence for the disease-causing allele. They may support the hypothesis by Sato et al. that the presence of $(TGGAA)_n$ repeats is important for the pathogenesis of SCA31. However, it is possible that a large insertion without $(TGGAA)_n$ repeats may have a pathological significance, requiring further investigation. The control individual with such insertion in this study may potentially develop cerebellar ataxia in the future, considering that SCA31 is a late-onset disease. The insertion sequences in SCA31 patients consist of (TAGAA), (TGGAA), and (TAAAA) penta-nucleotide repeats of variable numbers [6], but the precise pathogenesis by the penta-nucleotide repeat insertion remains unclear in SCA31. Further detailed characterization of the inserted sequence and data on genotype–phenotype correlation will be needed.

Acknowledgements We are grateful to the clinicians who provided us with information on their patients, and the patients and their families who participated in this study. This work was supported in part by a Grant-in-Aid for Science Research from the Ministry of Education, Science and Culture, Japan (KY and NM); a grant from the Research Committee for Ataxic Diseases, the Ministry of Health, Labour, and Welfare, Japan (KY); and a grant from the Ministry of Health, Labour, and Welfare, Japan (NM).

References

1. Takashima M, Ishikawa K, Nagaoka U, Shoji S, Mizusawa H (2001) A linkage disequilibrium at the candidate gene locus for 16q-linked autosomal dominant cerebellar ataxia type III in Japan. J Hum Genet 46:167–171. doi:10.1007/s100380170083
2. Li M, Ishikawa K, Toru S, Tomimitsu H, Takashima M, Goto J et al (2003) Physical map and haplotype analysis of 16q-linked autosomal dominant cerebellar ataxia (ADCA) type III in Japan. J Hum Genet 48:111–118. doi:10.1007/s100380300017
3. Hirano R, Takashima H, Okubo R, Tajima K, Okamoto Y, Ishida S et al (2004) Fine mapping of 16q-linked autosomal dominant cerebellar ataxia type III in Japanese families. Neurogenetics 5:215–221. doi:10.1007/s10048-004-0194-z
4. Ishikawa K, Toru S, Tsunemi T, Li M, Kobayashi K, Yokota T et al (2005) An autosomal dominant cerebellar ataxia linked to chromosome 16q22.1 is associated with a single-nucleotide substitution in the 5′ untranslated region of the gene encoding a protein with spectrin repeat and rho guanine-nucleotide exchange-factor domains. Am J Hum Genet 77:280–296. doi:10.1086/432518
5. Amino T, Ishikawa K, Toru S, Ishiguro T, Sato N, Tsunemi T et al (2007) Redefining the disease locus of 16q22.1-linked autosomal dominant cerebellar ataxia. J Hum Genet 52:643–649. doi:10.1007/s10038-007-0154-1
6. Sato N, Amino T, Kobayashi K, Asakawa S, Ishiguro T, Tsunemi T et al (2009) Spinocerebellar ataxia type 31 is associated with "inserted" penta-nucleotide repeats containing (TGGAA)n. Am J Hum Genet 85:1–14. doi:10.1016/j.ajhg.2009.09.019
7. Ouyang Y, Sakoe K, Shimazaki H, Namekawa M, Ogawa T, Ando Y et al (2006) 16q-linked autosomal dominant cerebellar ataxia: a clinical and genetic study. J Neurol Sci 247:180–186. doi:10.1016/j/jns.2006.04.009
8. Onodera Y, Aoki M, Mizuno H, Warita H, Shiga Y, Itoyama Y (2006) Clinical features of chromosome 16q22.1 linked autosomal dominant cerebellar ataxia in Japanese. Neurology 67:1300–1302
9. Nozaki H, Ikeuchi T, Kawakami A, Kimura A, Koide R, Tsuchiya M et al (2007) Clinical and genetic characterizations of 16q-linked autosomal dominant spinocerebellar ataxia (AD-SCA) and frequency analysis of AD-SCA in the Japanese population. Mov Disord 22:857–862. doi:10.1002/mds.21443
10. Basri R, Yabe I, Soma H, Sasaki H (2007) Spectrum and prevalence of autosomal dominant spinocerebellar ataxia in Hokkaido, the northern island of Japan: a study of 113 Japanese families. J Hum Genet 52:848–855. doi:10.1007/s10038-007-0182-x
11. Hayashi M, Adachi Y, Mori M, Nakano T, Nakashima K (2007) Clinical and genetic epidemiological study of 16q22.1-linked autosomal dominant cerebellar ataxia in western Japan. Acta Neurol Scand 116:123–127. doi:10.1111/j.1600-0404.2007.00815.x
12. Wieczorek S, Arning L, Alheite I, Epplen JT (2006) Mutations of the *puratrophin-1* (*PLEKHG4*) gene on chromosome 16q22.1 are not a common genetic cause of cerebellar ataxia in a European population. J Hum Genet 51:363–367. doi:10.1007/s10038-006-0372-y
13. Ohata T, Yoshida K, Sakai H, Hamanoue H, Mizuguchi T, Shimizu Y et al (2006) A −16C>T substitution in the 5′ UTR of the *puratrophin-1* gene is prevalent in autosomal dominant cerebellar ataxia in Nagano. J Hum Genet 51:461–466. doi:10.1007/s10038-006-0385-6
14. Shimizu Y, Yoshida K, Okano T, Ohara S, Hashimoto T, Fukushima Y et al (2004) Regional features of autosomal-dominant cerebellar ataxia in Nagano: clinical and molecular genetic analysis of 86 families. J Hum Genet 49:610–616. doi:10.1007/s10038-004-0196-6
15. Yoshida K, Shimizu Y, Morita H, Okano T, Sakai H, Ohata T et al (2009) Severity and progression rate of cerebellar ataxia in 16q-linked autosomal dominant cerebellar ataxia (16q-ADCA) in the endemic Nagano area of Japan. Cerebellum 8:46–51. doi:10.1007/s12311-008-0062-8

Epilepsy Research (2009) 87, 299–301

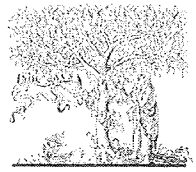

journal homepage: www.elsevier.com/locate/epilepsyres

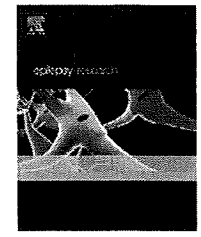

SHORT COMMUNICATION

Neuroepidemiology of West syndrome and early infantile epileptic encephalopathy in Miyagi Prefecture, Japan

Naomi Hino-Fukuyo[a,1], Kazuhiro Haginoya[a,b,*], Kazuie Iinuma[a,c,2], Mitsugu Uematsu[a,1], Shigeru Tsuchiya[a,1]

[a] *Department of Pediatrics, Tohoku University School of Medicine, 1-1 Seiryo-machi, Aoba-ku, Sendai 980-8574, Japan*
[b] *Department of Pediatric Neurology, Takuto Rehabilitation Center for Children, 20 Shikaotsu, Yumoto, Akiu-machi, Taihaku-ku, Sendai 982-0241, Japan*
[c] *Ishinomaki Red-Cross Hospital, Saidousita 71, Hebita, Ishinomaki 986-8522, Japan*

Received 19 August 2009; received in revised form 16 September 2009; accepted 20 September 2009
Available online 13 October 2009

KEYWORDS
West syndrome;
Early infantile epileptic encephalopathy;
Epidemiology;
Incidence;
Infantile spasms

Summary To compare the incidence of West syndrome (WS) and early infantile epileptic encephalopathy (EIEE) in Miyagi Prefecture, Japan, we studied retrospectively the medical records of cases involving WS or EIEE for the period 2000–2005. During this period, 45 children developed WS and one child was diagnosed with EIEE. The estimated incidence rates of WS and EIEE were 4.2 per 10,000 live births (95% CI, 3.0–5.5) and 0.1 per 10,000 live births (95% CI, 0–0.3), respectively. The occurrence of EIEE was one-fortieth that of WS.

Introduction

West syndrome (WS) and early infantile epileptic encephalopathy (EIEE) are both age-dependent catastrophic forms of epileptic encephalopathy. WS is an epileptic encephalopathy with variable etiology that consists of the triad of infantile spasms, arrest or regression of psychomotor development, and a specific electroencephalogram (EEG) pattern of hypsarrhythmia. EIEE is a specific epileptic syndrome with its onset mainly in the neonatal period, and it has many clinico-electrical characteristics, of which age dependency and progressive change are specific.

* Corresponding author at: Department of Pediatrics, Tohoku University School of Medicine, 1-1 Seiryo-machi, Aoba-ku, Sendai 980-8574, Japan. Fax: +81 22 717 7287.
E-mail addresses: naomi-h@zc4.so-net.ne.jp (N. Hino-Fukuyo), khaginoya@silk.ocn.ne.jp (K. Haginoya), kiinuma@ishinomaki.jrc.or.jp (K. Iinuma), uematsu@bk9.so-net.ne.jp (M. Uematsu), tsuchiya@idac.tohoku.ac.jp (S. Tsuchiya).
[1] Fax: +81 22 717 7287.
[2] Fax: +81 22 596 0122.

0920-1211/$ – see front matter © 2009 Elsevier B.V. All rights reserved.
doi:10.1016/j.eplepsyres.2009.09.012

Table 1 Reported incidence rates of West syndrome.

Authors	Published year	Country	Population	Rate (per 1000)
Riikonen and Donner	1979	Finland	260,777	0.42 (1960–1966) (live births) 0.38 (1967–1971) (live births) 0.42 (1973–1976) (live births)
Hauser et al.	1991	USA		0.11 (1940–1980) (live births)
Ludvigsson et al.	1994	Iceland	43,097	0.3 (1981–1990) (live births)
Sidenvall and Eeg-Olofsson	1995	Sweden	125,364	0.45 (1987–1991) (–1 year)
Rantala and Putkonen	1999	Finland		0.41 (1976–1993) (live births)
Trevathan et al.	1999	USA	69,199	0.29 (1975–1977) (live births)
Matsuo et al.	2001	Japan	148,999	0.31 (1989–1998) (live births)
Lee and Ong	2001	Singapore	43,664	0.31 (1998–1999) (live births)
Hwang	2001	Korea	600,000	0.25 (1997–2000) (live births)
Brna et al.	2001	Canada		0.307 (1978–1998) (live births)
Primec et al.	2002	Slovenia		0.026 (1985–1995) (live births)
Chen et al.	2004	Taiwan	33,363	0.06 (1985–1997) (live births)
Present report	2009	Japan	105,335	0.42 (2000–2005) (live births)

Population-based surveys of WS have been undertaken repeatedly in Japan (Oka et al., 2001; Matsuo et al., 2001) and in other countries, but no study has examined the incidence of EIEE. This prompted us to compare the incidence of WS and EIEE in Miyagi Prefecture, Japan.

Method

We studied patients with WS and EIEE who lived in Miyagi Prefecture when their illness began between 1 November 2000 and 30 September 2005. First, in February 2006, we sent inquiry forms to one university hospital (our hospital), 24 hospitals with a pediatrics department, four pediatric clinics, and three institutions for physically disabled children located in Miyagi Prefecture. These hospitals and clinics covered all of the pediatric neurology practice in Miyagi Prefecture. Then, we identified eligible cases from medical records. We used the cumulative incidence rather than rate to indicate the occurrence of WS among children in the birth cohort (Commission on Epidemiology and Prognosis, International League Against Epilepsy, 1993). The diagnostic criteria for WS followed Ohtsuka (1998) and included: (a) infantile spasms; (b) arrest or regression of psychomotor development; (c) a characteristic EEG pattern called hypsarrhythmia; (d) onset of seizures in early infancy, frequent association with partial seizures and atypical hypsarrhythmia; and (e) spasms in series after age 2 years (late-onset WS). We defined EIEE using the following criteria by Ohtahara and Yamatogi (2006): (a) onset of seizures within 1 month of birth, (b) tonic spasms with or without clustering while both awake and asleep, (c) continuous suppression bursts while both awake and asleep, and (d) a poor outcome with severe psychomotor retardation. We obtained a 100% response to our inquiry forms. Between 1 November 2000 and 30 September 2005, 105,335 babies were born according to Miyagi Prefecture demographic statistics.

Results

In Miyagi Prefecture, 45 children (18 boys and 27 girls) developed WS and one child was diagnosed with EIEE between 1 November 2000 and 30 September 2005. The late-onset WS was not found in the present study. The estimated incidence rates of WS and EIEE were 4.2 per 10,000 live births (95% CI, 3.0–5.5) and 0.1 per 10,000 live births (95% CI, 0–0.3), respectively.

Discussion

The main purpose of this population-based epidemiological study on WS and EIEE was to clarify the incidence rates of

Table 2 Reported prevalence rates of West syndrome.

Authors	Published year	Country	Population	Age distribution (year)	Rate (per 1000)
Doose and Sitepu	1983	Germany	37,691	0–8	0.47
Ishida	1985	Japan	61,872	0–2	0.16
Wendt et al.	1985	Finland	12,058	0–14	0.6
Joensen	1986	Denmark	43,609	All ages	0.09
Doerfer and Wasser	1987	Germany	20,132	0–14	0.15
Tsuboi	1988	Japan	17,044	At age 3 years	0.17
Cowan et al.	1989	USA	246,047	0–19	0.19
Bobo et al.	1994	USA	216,000	0–2	0.1
Oka et al.	1997	Japan	37,085	0–2	0.16
Trevathan et al.	1999	USA	89,534	At age 10 years	0.2
Chen et al.	2004	Taiwan	3,064,804	0–9	0.046